

DISSECTING THE CROSSTALK BETWEEN INHIBITORY RECEPTOR
SIGNALING AND THE T CELL RECEPTOR IN NATURAL KILLER CELLS

by

Ebru Zeynep Ergün

B.S., Genetics and Bioengineering, Yeditepe University, 2019

Submitted to the Institute for Graduate Studies in
Science and Engineering in partial fulfillment of
the requirements for the degree of
Master of Science

Graduate Program in Molecular Biology and Genetics
Boğaziçi University

2022

ACKNOWLEDGEMENTS

I would like to start by extending my gratitudes to my supervisor, Dr. Tolga Sütli. Throughout my master's studies he has been an incredibly valuable guide who helped me to think in a creative and scientific perspective. He has been extremely patient, and I will never forget his guidance.

I would also like to thank my jury members Prof. Batu Erman and Prof. Günnur Deniz for accepting to be on my committee and sharing their experiences and valuable perspectives with me for my project.

During these 3 years, I have made incredible friends. I want to thank all the Sütli Lab members: Elif Çelik, Mertkaya Aras, Zeynep Sena Karahan, Serra Özarı, Cevriye Pamukcu, Gözde Özcan, Ayşegül Durgun, Bahar Orhan, Eren Can Ekşi, Elif Ayşenur Karay, and Betül Çakıcı. To all our lab's undergraduate students, thank you so much for your help, especially for the final times of my thesis. I appreciate your helps in making those hectic experiment days a bit easier. Also, within the Boğaziçi University Molecular Biology and Genetics department there are many people who have helped through my struggles: Efe Elbeyli, Ulduz Sobhi-Afshar, İlke Süder, Davod Khalafkhany, and Emre Pekbilir. Thank you to all these amazing people, this would not be this easy if you were not there for me.

Now, I would like to express my special thanks to a few people, which would lead to a very teary few passages as everyone knows me expects. Zeynep Sena Karahan, like you have said, you are my lab twin. You have been there for me all along the way, and I can only hope that I have been there for you as well. We have shared amazing memories together through this journey and I could not choose a better partner in lab, thank you so much. Next comes Elif Çelik, who worked with me almost as much as me, lost sleep for the sake of me during this thesis (and almost for everyone in the lab). I could not thank you enough, for smoothing everything out and making them seem achievable. Also, Cevriye Pamukcu, who could not be here at the final times of

my thesis but was an amazing tutor during my time in the Sütlü Lab. Thank you so much for sharing your experiences and valuable tricks I will continue to use. I would also like to thank Efe Elbeyli, who has helped me along the way both scientifically and emotionally. I am so happy to have such an amazing person by my side which I desperately needed to get through this without a breakdown. Thank you for believing me and being there for me.

Lastly, I want to thank my family and friends because one needs to take a step back from this scientific journey to get through it, and these people who are outside the lab helped me to carry on in the lab. Aybüke and Şüheda, thank you for believing in me and being such supportive friends. I want to thank my family, my sister, mother, father, and my cat Loki. But my special thanks go to my dearest sister Tuba. She has always been with me, supported me, believed in me when I did not. She is the biggest cheerleader I have, and I love her so much.

ABSTRACT

DISSECTING THE CROSSTALK BETWEEN INHIBITORY RECEPTOR SIGNALING AND THE T CELL RECEPTOR IN NATURAL KILLER CELLS

Killer-cell immunoglobulin-like receptors (KIRs) are among the most prominent receptors regulating NK cell development and function. Most KIR ligands are the MHC class I molecules found on target cells. KIRs are responsible for NK cell licensing which is required for the NK cell to kill and differentiate self from non-self. Adoptive cell therapy based on T cell transfer relies on T cell receptor (TCR) or chimeric antigen receptor (CAR). However, with the TCR-T cells, the most important challenge is mispairing of transferred TCR chains with the endogenous TCR chains. Recently, TCR modification of NK cells has been applied as a solution to the mispairing of TCR chains in T cells. NK cells, with their similar downstream signaling machinery to T cells, can replace T cells in TCR-T cell therapy. These modifications were performed on NK92 cells that lacks inhibitors. This study tries to elucidate how inhibitory signals interfere with TCR signaling.

TCR-NK cells against the melanoma-associated antigen Tyrosinase, have been transduced with KIR2DL1 coding lentiviral particles for stable KIR2DL1 expression. The function of the TCR-NK-KIR2DL1 cells was measured against K562 or melanoma cells A375 and A375Tyr. The degranulation of TCR-NK-KIR2DL1 cells was observed to be slightly higher independent from the antigen. Similarly, real-time cell analysis showed the cytotoxicity induced by KIR2DL1 did not show a significant difference. Cytokine secretion showed there might be a KIR2DL1-mediated TNF- α decrease against A375Tyr cells, but not the same for IFN- γ secretion. Phospho-protein analysis of TCR-NK-KIR2DL1 showed a decrease in PLC γ 1 and Erk1/2 levels against all targets.

ÖZET

DOĞAL ÖLDÜRÜCÜ HÜCRELERDE İNHİBİTÖR RESEPTÖR SİNYALİ İLE T HÜCRESİ RESEPTÖRÜ ARASINDAKİ İLETİŞİMİN ARAŞTIRILMASI

Doğal öldürücü hücre immünoglobulin benzeri reseptörler (KIR), NK hücre gelişimini ve fonksiyonunu düzenleyen en belirgin reseptörler arasındadır. KIR ligandlarının çoğu, hedef hücrelerde bulunan MHC sınıf I molekülleridir. KIR'ler, NK hücresinin öldürebilmesi ve kendinden olmayana ayırt etmesi için gerekli olan NK hücresi lisanslamasından sorumludur. T hücre transferine dayalı adoptif hücre tedavisi, T hücre reseptörüne (TCR) veya kimerik antijen reseptörüne (CAR) dayanır. TCR-T hücreleri ile ilgili en önemli zorluk, transfer edilen TCR zincirlerinin endojen TCR zincirleri ile yanlış eşleşmesidir. Son zamanlarda NK hücrelerinin TCR modifikasyonu, T hücrelerindeki yanlış eşleşmeye bir çözüm olarak uygulanmıştır. NK hücreleri, T hücrelerine benzer aşağı akış sinyalleriyle TCR-T hücre tedavisinde T hücrelerinin yerini alabilir. Bu modifikasyonlar, inhibitörleri olmayan NK92 hücreleri üzerinde gerçekleştirilmiştir. Bu çalışma, inhibitör sinyallerin TCR sinyaline nasıl müdahale ettiğini açıklamaya çalışır.

Melanoma ilişkili antijen Tyrosinase'e hedeflenen TCR-NK hücreleri stabil KIR2-DL1 ekspresyonu için KIR2DL1 lentiviral partikülleriyle transdükte edildi. Hücrelerin işlevi, K562 veya melanom hücreleri A375 ve A375Tyr'e karşı ölçüldü. Antijenden bağımsız olarak TCR-NK-KIR2DL1 hücrelerinin degranülasyon kapasitelerinde artış gözlemlendi. Gerçek zamanlı hücre analiziyle KIR2DL1'in sitotoksitede bir fark yaratmadığı gözlemlendi. Sitokin salgılanmasında A375Tyr hücrelerine karşı KIR2DL1 aracılı TNF- α 'da düşüş gözlenirken, IFN- γ 'da değişim gözlenmedi. Fosfoprotein analizi tüm hedeflere karşı efektör hücrelerin PLC γ 1 ve Erk1/2 seviyelerinde bir düşüş gösterdi.

TABLE OF CONTENTS

ACKNOWLEDGEMENTS	iii
ABSTRACT	v
ÖZET	vi
LIST OF FIGURES	x
LIST OF TABLES	xiii
LIST OF SYMBOLS	xiv
LIST OF ACRONYMS/ABBREVIATIONS	xv
1. INTRODUCTION	1
1.1. The Immune System	1
1.2. T Cells	4
1.2.1. TCR and T Cell Mediated Target Recognition	5
1.3. Natural Killer Cells	7
1.3.1. NK Cell Mediated Target Recognition	8
1.3.1.1. NK Cell Receptors	9
1.3.1.2. Killer-cell Immunoglobulin Like Receptors	12
1.4. TCR-NK Cells	14
2. AIM	17
3. MATERIALS AND METHODS	18
3.1. Materials	18
3.1.1. Chemicals	18
3.1.2. Equipment	18
3.1.3. Buffers and Solutions	18
3.1.4. Growth Media	19
3.1.5. Commercial Kits	20
3.1.6. Enzymes	20
3.1.7. Antibodies	21
3.1.8. Bacterial Strains	21
3.1.9. Mammalian Cell Lines	21
3.1.10. Plasmids and Oligonucleotides	22

3.2. Methods	23
3.2.1. Bacterial Cell Culture	23
3.2.2. Mammalian Cell Culture	24
3.2.3. Design and Cloning	25
3.2.4. Lentiviral Particle Production	29
3.2.5. Lentiviral Transduction of NK-92 Cells	30
3.2.6. Flow Cytometry	30
3.2.7. Degranulation of TCR-NK Cells	31
3.2.8. Real-time Cell Analysis of TCR-NK Cells	31
3.2.9. Intracellular TNF- α and IFN- γ Staining	32
3.2.10. Statistical Analysis	32
4. RESULTS	33
4.1. Cloning of CD3 and Receptor Vectors	33
4.1.1. Cloning of LeGO-DGE-IRES-puro	33
4.1.2. Confirmation of LeGO-KIR2DL1-iT2	35
4.2. Lentiviral Vector Productions	36
4.3. Genetic Modification of NK92-TyrTCR Cells	37
4.3.1. Genetic Modification of NK-92-TCR Cells with CD3 Subunits	37
4.4. Genetic Modification of NK-92TCR(DGE) Cells with KIR2DL1	39
4.4.1. FACS Sorting of KIR2DL1 Expressing NK-92TCR(DGE) Cells and Surface Analysis	39
4.5. Functionality of TCR-NK KIR2DL1 Cells	40
4.5.1. Degranulation of Antigen-specific TCR-NK KIR2DL1 Cells	40
4.5.2. Cytotoxic Activity of TCR-NK KIR2DL1 Cells	43
4.5.3. TNF- α and IFN- γ Secretion of TCR-NK KIR2DL1 Cells	47
4.5.4. Western Blot Analysis of Phospho-proteins in TCR-NK KIR2DL1 Cells	50
5. DISCUSSION	52
6. REFERENCES	56
APPENDIX A: CHEMICALS	68
APPENDIX B: EQUIPMENTS	70

APPENDIX C: ADAPTATIONS	72
APPENDIX D: PLASMID MAPS	73
APPENDIX E: DNA LADDER	79
APPENDIX F: PROTEIN LADDER	80

LIST OF FIGURES

Figure 1.1.	Hematopoetic stem cell lineage.	2
Figure 1.2.	TCR downstream signaling.	6
Figure 1.3.	NK cell receptors	7
Figure 1.4.	Target recognition of NK cell mediated cytotoxicity.	9
Figure 1.5.	NK cell signaling pathways.	11
Figure 4.1.	Gel images of predicted and actual colony PCR results of LeGO-DGE-IRES _{puro}	33
Figure 4.2.	Gel images of predicted and actual restriction digestion results of LeGO-DGE-IRES _{puro} vectors	34
Figure 4.3.	Flow cytometry analysis of CD3 ϵ surface expression on 293FT cells, co-transfected with TCR $\alpha\beta$ chains.	35
Figure 4.4.	Gel images of predicted and actual control digestion results of LeGO-KIR2DL1-iT2	36
Figure 4.5.	Lentiviral constructs for CD3 subunits and KIR2DL1.	37
Figure 4.6.	Flow cytometry results of transduction of NK-92TCR cells with CD3 subunits, followed by puromycin selection.	38

Figure 4.7.	KIR2DL1 surface expression of NK-92TCR(DGE) cells assessed by flow cytometry.	39
Figure 4.8.	Degranulation of NK-92TCR(DGE)-KIR2DL1 cells.	40
Figure 4.9.	Degranulation of NK-92TCR(DGE)-KIR2DL1 cells for 1 hour. . .	41
Figure 4.10.	Degranulation of KIR2DL1 expressing cells against A375Tyr cells at different time points.	42
Figure 4.11.	Second time-point degranulation assay against A375Tyr cells. . . .	43
Figure 4.12.	Real-time cell analysis of different effector cells against both A375 and A375Tyr cells.	44
Figure 4.13.	1-to-6-hour timepoints of cell indexes which were baseline-corrected to no effector cell indexes at each hour.	44
Figure 4.14.	RTCA analysis of the effector cells against A375 and A375Tyr at 0.1:10 E:T ratio.	45
Figure 4.15.	1-to-6-hour timepoints of cell indexes which were baseline-corrected to no effector cell indexes at each hour.	45
Figure 4.16.	RTCA analysis of the effector cells against A375 and A375Tyr at 0.3:10 E:T ratio.	46
Figure 4.17.	1-to-6-hour timepoints of cell indexes which were baseline-corrected to no effector cell indexes at each hour.	46
Figure 4.18.	TNF- α expression levels in A375Tyr stimulated effector cells. . .	47

Figure 4.19. Bar graph representation of TNF- α secretion.	48
Figure 4.20. IFN- γ expression levels in A375Tyr stimulated effector cells.	49
Figure 4.21. Bar graph representation of IFN- γ secretion.	50
Figure 4.22. Phospho-PLC γ 1 expression levels in stimulated effector cells.	51
Figure 4.23. PPhospho-Erk1/2 and total Erk expression levels in stimulated effector cells.	51
Figure D.1. The plasmid map of LeGO-DGEiTCR.	73
Figure D.2. The plasmid map of LeGO-DGE-IRESpuro.	74
Figure D.3. The plasmid map of LeGO-KIR2DL1-iT2	75
Figure D.4. The plasmid map of pMDLg/gpRRE.	76
Figure D.5. The plasmid map of pRSV-Rev.	77
Figure D.6. The plasmid map of pCMV-VSV-G.	78
Figure E.1. DNA ladder	79
Figure F.1. Protein ladder	80

LIST OF TABLES

Table 1.1.	KIRs and their ligands	14
Table 3.1.	List of commercial kits	20
Table 3.2.	List of enzymes	20
Table 3.3.	List of antibodies	21
Table 3.4.	List of plasmids	22
Table 3.5.	List of oligonucleotides	23
Table 4.1.	Table of viral titers	37
A.1	Chemicals used in this study	68
B.1	Equipments used in this study	70

LIST OF SYMBOLS

g	Gram
L	Liter
M	Molar
mL	Mililiter
mM	Milimolar
ng	Nanogram
α	Greek letter alpha representing different protein subunits
β	Greek letter beta representing different protein subunits
δ	Greek letter delta representing different protein subunits
γ	Greek letter gamma representing different protein subunits
ϵ	Greek letter epsilon representing different protein subunits
κ	Greek letter kappa representing different protein subunits
ζ	Greek letter zeta representing different protein subunits
μg	Microgram
μl	Microliter
μM	Micromolar
μm	Micrometer

LIST OF ACRONYMS/ABBREVIATIONS

ADCC	Antibody-Dependent Cellular Cytotoxicity
ANOVA	Analysis Of Variance
CAR	Chimeric Antigen Receptor
CLIP	Class II-associated Invariant chain Peptide
DAMP	Damage-Associated Molecular Patterns
DAP10/12	DNAX Activating Protein of 10 kDA/12 kDA
DNA	Deoxyribonucleic Acid
ERK	Extracellular signal-Regulated Kinase
FcεRI-γ	High-affinity IgE receptor
HLA	Human Leukocyte Antigen
ICAM-1	Intracellular Adhesion Molecule 1
IFN-γ	Interferon γ
IL-2/4/5/13/17	Interleukin 2/4/5/13/17
IP3	Inositol Triphosphate
ITAM	Immunoreceptor Tyrosine-based Activation Motif
ITIM	Immunoreceptor Tyrosine-based Inhibition Motif
IU	International Unit
KIR	Killer-cell Immunoglobulin-like Receptor
LAT	Linker for Activation of T cells
LFA-1	Lymphocyte Function-associated Antigen 1
MAPK	Mitogen-Activated Protein Kinase
MHC	Major Histocompatibility Complex
NFAT	Nuclear Factor of Activated T-cells
NF-κB	Nuclear Factor Kappa-light-chain-enhancer of activated B cells
NK	Natural Killer cells
PAMP	Pathogen-Associated Molecular Pattern
PCR	Polymerase Chain Reaction
PI3K	Phosphatidylinositol-3-Kinase

PLC γ	Phospholipase C γ
PRR	Pattern Recognition Receptors
RAG1/2	Recombination Activating Gene 1/2
RNA	Ribonucleic Acid
SHIP	Src Homology 2 domain containing Inositol Polyphosphate 5-Phosphatase
SHP1/2	Src Homology region 2 domain-containing Phosphatase-1/2
TAP	Transporter Associated with Antigen Processing
TCR	T Cell Receptor
TNF- α	Tumour Necrosis Factor α
β 2m	β 2 microglobulin

1. INTRODUCTION

1.1. The Immune System

The immune system comprises many organs, cells, and molecules that protect the host from foreign agents. Based on the response's specificity and speed, the immune system is generally divided into two: the innate immune system and the adaptive immune system. While innate immunity is non-specific and fast, adaptive immunity is highly specific and slower (Parkin & Cohen, 2001).

Charles Janeway's pattern recognition theory has built the foundation of the concept of innate immunity. He stated the existence of pattern recognition receptors (PRRs) found in antigen-presenting cells, which were evolutionarily conserved and can recognize common patterns in microorganisms (Janeway, 1989). These common patterns are named pathogen-associated molecular patterns or PAMPs. A few examples of PAMPs are bacterial DNA, double-stranded RNA, and bacterial lipopolysaccharides. The innate immune system has many types of cells that express these germ-line encoded PRRs; macrophages, dendritic cells, natural killer cells, mast cells, neutrophils, and eosinophils (1.1). When these cells are triggered through PAMP recognition, they immediately respond and later proliferate (Janeway & Medzhitov, 2002; Medzhitov & Janeway, 2009). While non-self-molecules carry PAMPs and create an immune response, it is also occasionally observed that a similar response can be mediated despite a lack of infection (Matzinger, 1994). This response is initiated by somewhat-self-molecules such as damaged or stressed cells, which are recognized through their DAMPs or danger-associated molecular patterns. DAMPs are also recognized through PRRs (Land, 2003).

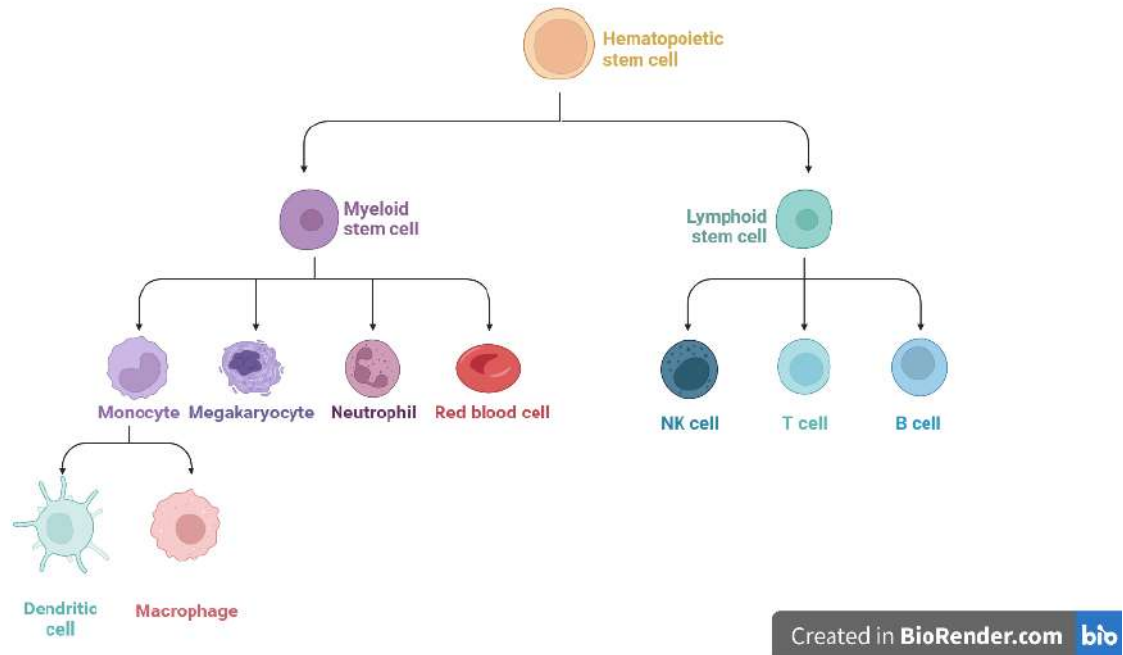


Figure 1.1. Hematopoietic stem cell lineage.

These PRRs that are present in innate immune cells enable the elucidation of a signal to activate adaptive immunity. The most prominent player in this role is dendritic cells, which express (Janeway & Medzhitov, 2002) PRRs to detect infection and initiate a response through triggering of adaptive immune cells such as T cells. Triggering of T cells through dendritic cells is also initiated via peptide:MHC presentation (Steinman & Witmer, 1978). This multifaceted response inducing mechanism of dendritic cells makes them an unexchangeable cell type (Palucka & Banchereau, 1999).

While innate immunity is extremely fast, it lacks specificity. Since innate recognition is germ-line coded, it has its limits. However, the adaptive immune system relies on B and T lymphocytes (Figure 1.1) to generate immune responses against specific antigens. The vast array of recognition receptors of these cells is generated through the somatic diversity of antigen receptor genes on the lymphocytes (Cooper & Alder, 2006).

Recognition of the antigen by the T cell receptor (TCR) requires the presence of the peptide derived from the antigen on a specific protein called major histocompatibility complex (MHC). This complex of proteins has two types: class I and II. While class I MHCs are found on all nucleated cells, class II MHCs are found on antigen-presenting cells, such as dendritic cells and macrophages of the innate immune system and B cells of the adaptive immune system (Wieczorek et al., 2017). In MHC I antigen presentation, peptides resulting from the degradation of intracellular antigens through nuclear or cytosolic proteasomes are transported to the endoplasmic reticulum by the transporter associated with antigen presentation (TAP), where they can reach the MHC I molecules. Accordingly, in the endoplasmic reticulum, MHC class I complex is assembled by a heavy and light chain (β 2-microglobulin, β 2m). This complex is not stable without the presence of a peptide inside the peptide-binding groove, so when the peptide insertion is successfully completed into the complex, now the stable peptide:MHC is released to cell surface (Kloetzel, 2004; Stern & Wiley, 1994). Similar to class I MHCs, class II MHC molecules follow a similar antigen presentation pathway, but with exogenous antigens. Peptide binding groove of MHC class II molecules is protected by invariant chain, Ii, in the absence of a peptide. Proteolysis of Ii leads to formation of class II invariant chain peptide or CLIP, which resides in the peptide binding groove. Dissociation of CLIP from MHC class II, and its translocation with the antigen peptide is mediated by HLA-DM proteins. Following the CLIP removal, and peptide binding, peptide:MHC II complex travels to cell surface (Germain & Margulies, 1993; Watts, 2004).

In addition to the diverse and specific nature of adaptive immune cells, they also possess memory functions. After their encounter with specific antigens, these lymphocytes turn into effector and memory cells. The immunological memory provided by the memory cells enables a faster response against an antigen when encountered a second time (Sprent & Tough, 1994).

1.2. T Cells

T lymphocytes, one of the two major cell types responsible for adaptive immunity, arise from bone marrow progenitors, similar to B cells. However, T cell precursors migrate to the thymus, unlike B cells, during their development. T lymphocytes undergo several stages in the thymus depending on their expression of different cell surface proteins and T-cell receptor (TCR) genes. These proteins include TCR complex proteins; CD3, $\alpha:\beta$ or $\gamma:\delta$ TCR chains, and CD4 and CD8 co-receptor proteins (B. v. Kumar et al., 2018).

During development, the first random rearrangement of TCR chains occurs where most of the developed T cells express $\alpha:\beta$ chains and further develop to express different cell-surface proteins. These cells are called double-negative at this stage due to their lack of co-receptor expression. Later, these cells express CD4 and CD8, called double-positive T cells. However, these cells express TCR genes at low levels. Therefore, when they meet self-peptide:MHC ligands, they lose either one of the co-receptors. Then these single-positive T cells leave the thymus as mature CD4 or CD8 positive T cells (Germain, 2002).

After their maturation into single-positive T cells, they are either cytotoxic T cells expressing CD8 or helper T cells expressing CD4. While CD8 positive T cells are restricted to recognize MHC class I molecules, CD4 positive T cells are restricted to recognize MHC class II molecules. Recognition of a peptide presented via MHC class II on professional antigen presenting cells like dendritic cells leads to activation of CD4 positive T cells, and recognition of a peptide presented via MHC class I on all nucleated cells can lead to activation of cytotoxic CD8 positive T cells. Helper T (Th) cells are then categorized into subtypes according to the cytokines they produce and have different properties. One subtype of Th cells is called Th1 cells, which are known to produce interferon- γ , TNF- α , and IL-2. The most prominent cytokine produced by Th1 cells is IFN- γ . It has important effects as a proinflammatory agent, such as increasing antigen presentation by MHC I and II and activating macrophages (Boehm et al., 1997; Mosmann et al., 1986; Raphael et al., 2015).

Th2 cells are mainly associated with allergy-related responses. They are known to secrete IL-4, -5, and -13. Additionally, they are responsible for class switching to some immunoglobulin isotypes and macrophage activation (Fallon et al., 2002). Another subtype of helper T cells is known for their production of IL-17, named Th17, which is responsible for regulating tissue inflammation (Park et al., 2005). Tregs, or regulatory T cells, are responsible for preventing autoimmunity by inhibiting T cell growth and cytokine secretion (Raphael et al., 2015).

Diverse response mediated through adaptive immunity is the result of clonal selection of the T lymphocytes (and B lymphocytes). Burnet's clonal selection theory states the expansion of a group of lymphocytes that are already present after encountering the specific antigen they were built to recognize (Burnet, 1957) With the clonal selection theory, it is known that these lymphocytes express their antigen receptors prior to an introduction with the antigen. Later, when the antigen interaction occurs, the clonal expansion starts, whereby the proliferation of the specific T cell clone is initiated (Adams et al., 2020).

1.2.1. TCR and T Cell Mediated Target Recognition

The vast diversity and specificity of adaptive immunity come from its cells' receptors that recognize antigens. Somatic rearrangement of both B cell receptors (immunoglobulins) and T cell receptors (TCR) is mediated by recombination-activating genes, RAG1 and RAG2. Antigen binding domains of these receptors are rearranged to create this diversity in a process called V(D)J recombination, where antigen receptor gene segments variable (V), diversity (D), and joining (J) are rearranged (Schatz & Ji, 2011).

The first signal required for T cell activation is initiated from the interaction between the peptide:MHC presented on dendritic cells with the TCR complex and its co-receptor (CD4 or CD8) (Reinherz, 2015; Reinherz et al., 1983). Another signal is the interaction between costimulatory molecules on dendritic cells and T cells at the immune synapse, such as B7/CD28 or ICAM-1/LFA-1 interactions (Anderson & Siahhaan,

2003). Signal-1 leads to phosphorylation events at the immunoreceptor tyrosine-based activation motifs (ITAMs) on CD3 subunits at the TCR complex and co-receptors, as seen in Figure 1.2

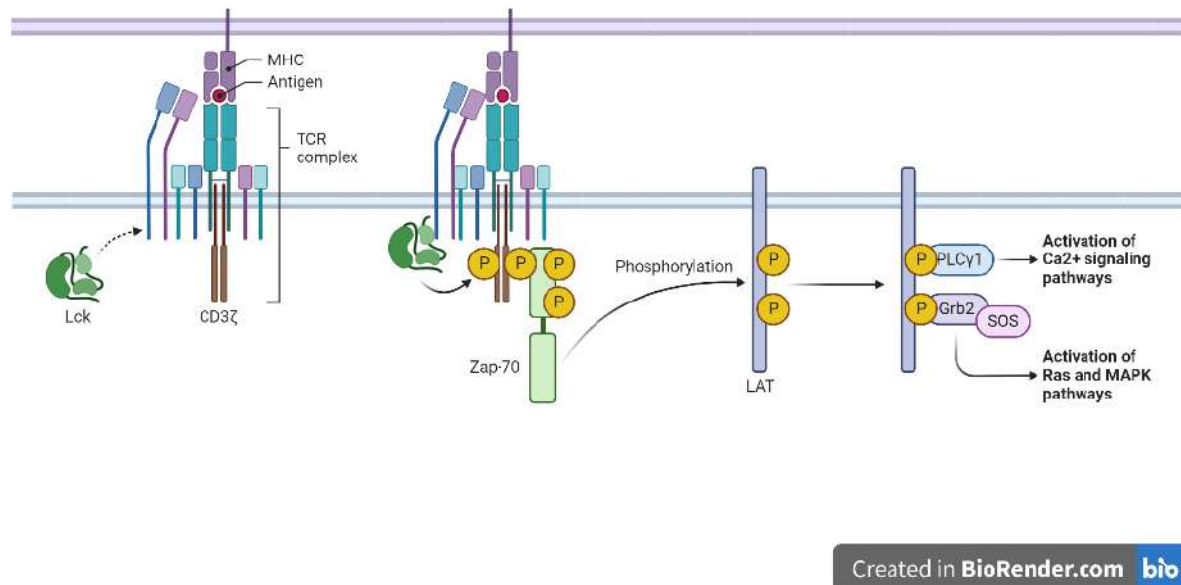


Figure 1.2. TCR downstream signaling.

The protein tyrosine kinases from the Src family, Lck, initiate phosphorylation. Then, another kinase, ZAP70, binds to ITAM, and its phosphorylation leads to its activation to phosphorylate SLP-76 and LAT adaptor proteins required for the signal relay. These adaptors regulate Ras and MAPK pathways, which are important in regulating proliferation-related genes (Cantrell, 2002; Genot & Cantrell, 2000). Additionally, phospholipase C- γ (PLC γ) phosphorylation resulting from peptide:MHC triggered TCR leads to activation of 1,4,5-inositol-triphosphate or IP₃, which is responsible for Ca²⁺ entry into the cytosol, which is extremely important in lymphocyte activation and cytokine production (Figure 1.2) (Feske, 2007; Lewis, 2001).

Activated cytotoxic T cells trigger apoptosis of the infected cell through perforin secretion, which results in pore formation in the infected cell and a serine protease called granzyme B (Trapani, 1995). On the other hand, activating CD4⁺ helper T

cells leads to the production of various cytokines required for many effector functions (Medzhitov, 2007).

1.3. Natural Killer Cells

T cells are known for their ability to recognize and respond to foreign antigens through the presentation on MHC molecules. However, they become unresponsive when MHC expression is lost or downregulated on the target cells.

This lack of recognition is compensated by one of the most critical members of innate immunity, natural killer (NK) cells. They are large granular lymphocytes known for their high cytotoxicity against tumour cells and virally infected cells without the need for antigen-specific receptors (Trinchieri, 1989; Vivier et al., 2008). Their cytotoxicity is balanced by many cell surface activating and inhibitory receptors as seen in Figure 1.3, and their function is determined through the shifts in this balance. The most important feature of these cells is their ability to recognize stressed cells apart from healthy cells (Vivier et al., 2004a). NK cells are built to recognize and respond to the absence of self-MHC molecules, which are found at low expression levels or absent in many tumours and virally infected cells (Kärre et al., 1986).

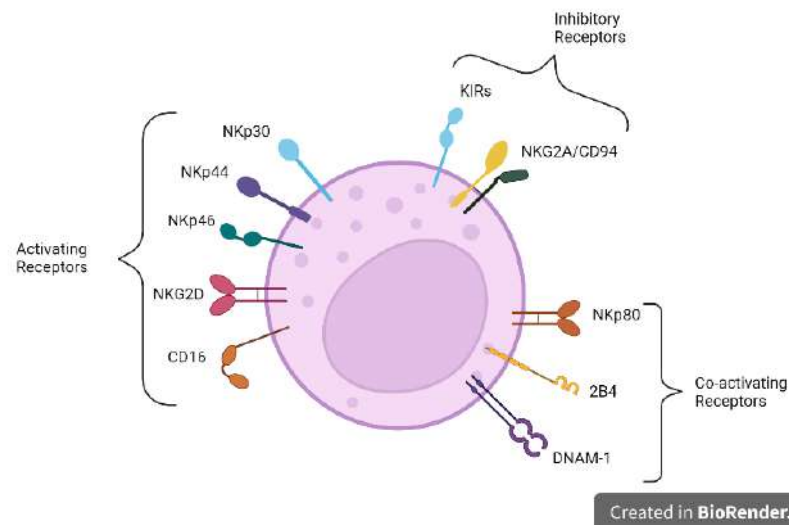


Figure 1.3. NK cell receptors

NK cells can circulate through the peripheral blood and can be found in many organs such as lymph nodes, spleen, and bone marrow. The basic definition of NK cell subsets are defined through the lack of CD3 expression and the presence of two surface receptors in humans: CD56 and CD16. Two main human NK cell subsets are CD3⁻CD56^{dim}CD16⁺ NK cells or CD3⁻CD56^{bright}CD16⁻ NK cells. CD56^{dim}CD16⁺ subset is known to be more cytotoxic when compared to the CD56^{bright}CD16⁻ subset, but the CD56^{bright} subset of NK cells can produce more cytokines upon activation. Most human peripheral blood NK cells belong to the CD56^{dim}CD16⁺ subset (M. A. Cooper et al., 2001; Hanna et al., 2004)

1.3.1. NK Cell Mediated Target Recognition

The outcome of ‘dynamic equilibrium’ between signals from activating and inhibitory receptors on the NK cell surface decides the response against a target cell. While cytotoxic T lymphocytes require the presence of an MHC ligand to respond, in some cases, MHC expression can be downregulated or absent. In this situation, cytotoxic T lymphocytes (CTLs) cannot produce a response (Hewitt, 2003). Unlike CTLs, NK cells are not MHC-restricted in terms of target recognition. However, the MHC molecules play a crucial role in determining NK cell responses. Inhibitory receptors on NK cells can recognize MHC class I molecules, and their triggering results in a shift in this dynamic equilibrium toward inhibition. In the absence of MHC class I molecules, NK cells cannot be inhibited; hence, the equilibrium shifts toward activation of the NK cell (Figure 1.4) (Topham & Hewitt, 2009). This clarifies the killing mechanism of NK cells, which is through recognition the “missing”, of information on the target cell, and is called missing-self recognition of NK cells (Ljunggren & Kärre, 1990).

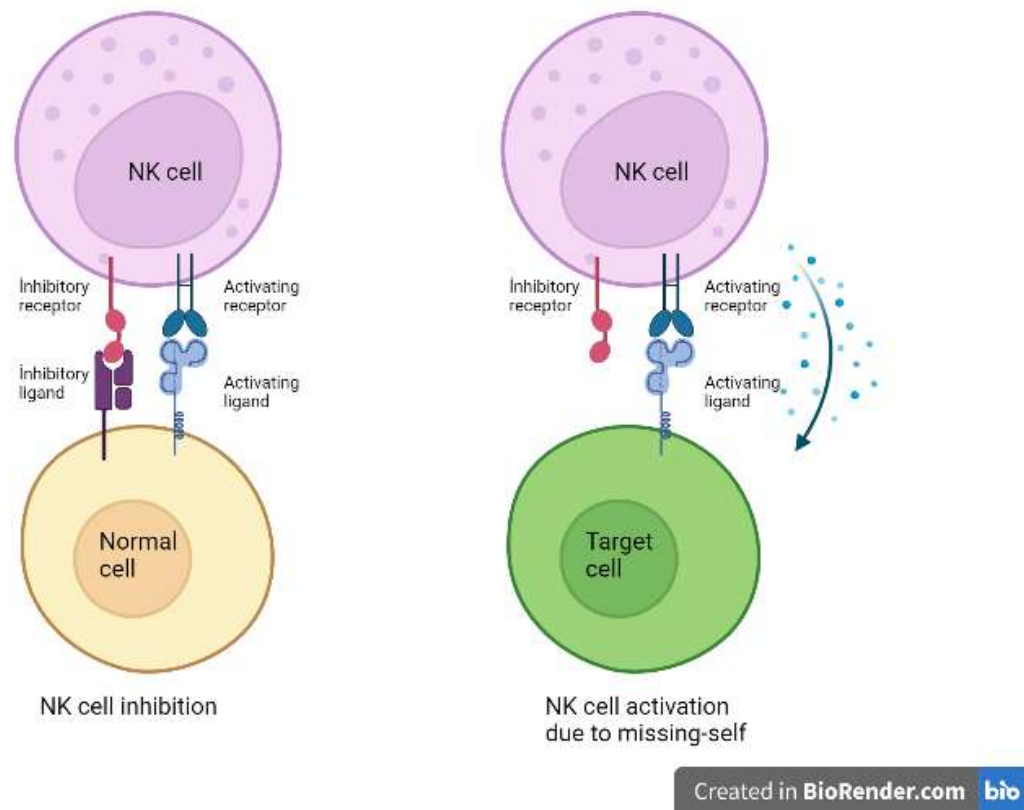


Figure 1.4. Target recognition of NK cell mediated cytotoxicity.

After the target cell binds to the NK cell, ligands on the target cell surface engage with the NK cell receptors to determine whether the NK cell remains attached to respond or detaches (Lanier, 2005). The response of NK cell to a target is like a CTL, through perforin and granzymes secretion (degranulation) and secretion of cytokines. These cytolytic proteins, perforin, and granzyme are found in cytolytic granules of NK cell cytoplasm. They are released at the immunological synapse upon activation, which results in target cell death (Moretta et al., 2002).

The recognition of the target can be further elucidated by explaining the many NK cell receptors, which will be given in detail in the next chapter.

1.3.1.1. NK Cell Receptors. Instead of one single antigen-specific receptor, NK cell function depends on a vast array of activating and inhibitory receptors. The trig-

gering of different activating receptors and their cumulative response results in effector activity of the NK cell. These receptors include NKG2D, CD16, activating killer immunoglobulin-like receptors (KIRs), and natural cytotoxicity receptors (NCRs). Different signaling adaptors of these receptors result in the initiation of various signaling pathways (Lanier, 2008).

NK cells express activating complexes on their surfaces formed by the association of different transmembrane adaptor peptides such as Fc ϵ RI- γ , DAP12, and CD3 ζ . These adaptors contain immunoreceptor tyrosine-based activation motifs (ITAMs) at their cytoplasmic region, with the sequence of (D/E)XXYXX(L/I)X6–8YXX(L/I). They either form homodimers (as in DAP12) or heterodimers (Fc ϵ RI- γ and CD3 ζ) through their small extracellular regions. Phosphorylation of ITAM residues through receptor-ligand engagement starts a signaling cascade similar to TCR signaling (Lanier, 2001; Lanier et al., 1998). Phosphorylation of the residues is dependent on many Src family kinases such as Lck, Fyn, and Src. Followed by phosphorylation, these residues recruit tyrosine kinases belonging to the Syk family like ZAP70 and Syk. Recruitment of these kinases leads to activation of many signaling intermediates such as phosphoinositide 3-kinase (PI3K), as well as PLC γ 1, PLC γ 2, Vav2, Vav3, and LAT. This phosphorylation cascade activates MAPK and ERK pathways and increases intracellular Ca²⁺ levels (Gross et al., 2008; Lanier, 2003). CD16 signaling is one of the most investigated modes of ITAM-mediated activation of NK cells, which occurs through either Fc ϵ RI- γ or CD3 ζ . This receptor signaling enables the recognition of antibody-coated cells, and the result of this pathway is called antibody-dependent cellular cytotoxicity (ADCC). Activation of this signaling pathway is very similar to TCR signaling. Activation of the nuclear factor of activated T cells (NFAT) is followed by cytokine production such as IFN- γ , leading to NK cell degranulation, which is similar to TCR-triggered responses in T cells (Lanier, 2003; Vivier et al., 2004b). Besides CD16, ITAM-associated receptors include activating KIRs, NKp30, NKp44, and NKp46. They either couple with DAP12 (KIRs, NKp44) or Fc ϵ RI- γ or CD3 ζ (NKp30, NKp46) (Medjouel Khelifi et al., 2022).

Another transmembrane adaptor peptide, DAP10, associated with the NKG2D receptor, is responsible for a somewhat different signaling pathway than ITAM mediated signaling. While ITAM-mediated signaling depends on Syk family kinases, DAP10-mediated signaling does not. Additionally, these two pathways differ in signaling intermediates they phosphorylate; while during ITAM-mediated signaling Vav2 and Vav3 are phosphorylated, DAP10-mediated signaling is responsible for phosphorylation of Vav1. Another difference between the two signals is that while ITAM-mediated signals lead to cytotoxicity and cytokine secretion, DAP10-mediated signals lack cytokine secretion (Vivier et al., 2004b).

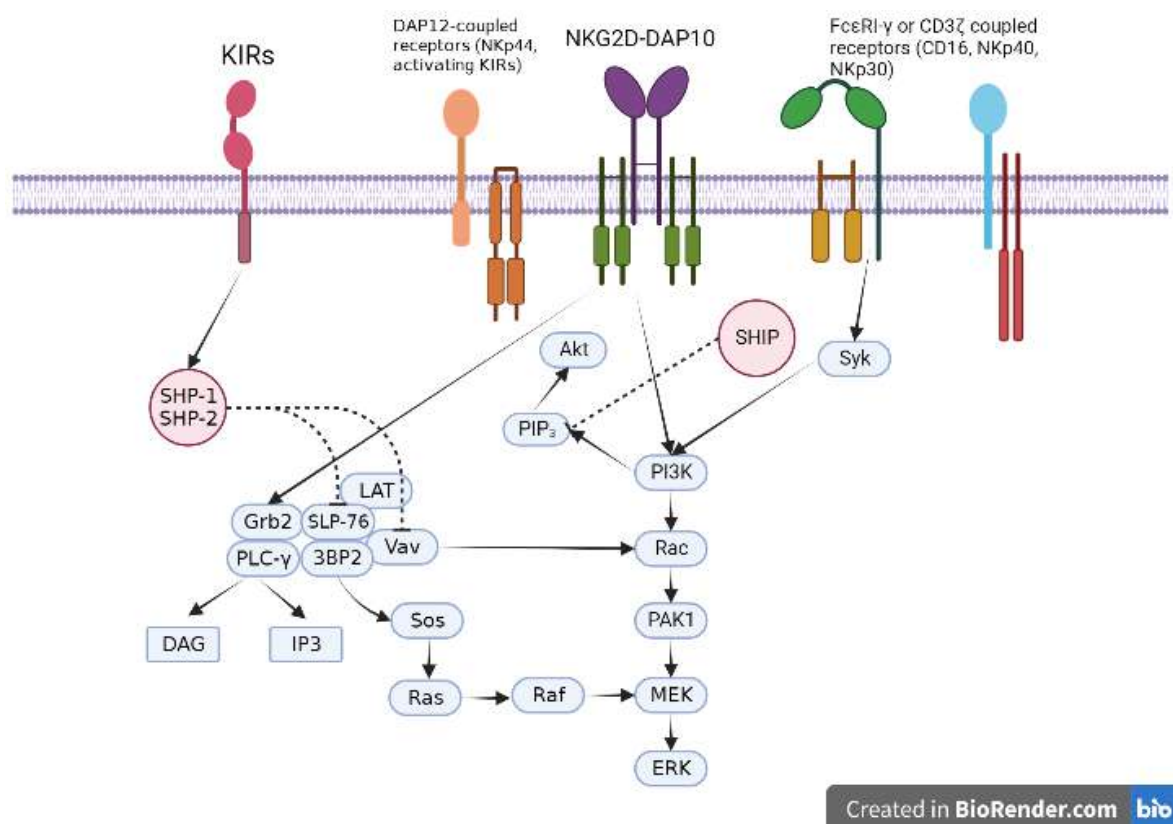


Figure 1.5. NK cell signaling pathways.

Although the two signalings have differences, the cytotoxicity pathway initiated by them is also very similar. Both signals activate Rac, leading to the activation of MAPK and ERK pathways, which results in NK cell degranulation (Jiang et al., 2000; Vivier et al., 2004b).

The counter-force required for the balancing these activation signals is given through many inhibitory receptors. Their ligands can be specifically MHC class I or non-MHC molecules. The most prominent group of inhibitory receptors are killer cell immunoglobulin-like receptors (KIRs), which will be further discussed in detail in the following chapter. However, another group of inhibitory receptors belong to C-type lectins, and are called NKG2A-CD94 receptors. With its ligand as non-classical MHC class I molecule, HLA-E, it acts as an inhibitory receptor to counteract the activating signals in both NK and T cells (Braud et al., 1998). Both KIRs and NKG2A-CD94 share common signaling motifs called immunoreceptor tyrosine-based inhibitory motifs (ITIMs) responsible for inhibitory signaling (S. Kumar, 2018; Lanier, 2008).

1.3.1.2. Killer-cell Immunoglobulin Like Receptors. The killer-cell immunoglobulin like receptors, or KIRs, are a group of surface receptors that have either activating or inhibitory functions on NK cells. They are characterized by their extracellular Ig-like domains and intracellular regions with different signaling motifs that define their function. The KIR locus is highly polymorphic, very similar to their ligands, MHC class I molecules.

KIR nomenclature is defined by the number of Ig-like domains and the length of intracellular regions. They are named either KIR2D or KIR3D, meaning they have 2 Ig-like domains or 3. Also, they can be named KIR2DS or KIR2DL, where S means the receptor has a short cytoplasmic tail, and L means it has a long cytoplasmic tail. The length of the cytoplasmic tail suggests whether the KIR is activating or inhibitory, where KIRs with short cytoplasmic tails are activating, and KIRs with long cytoplasmic tails are inhibitory. Additionally, they have a CD number CD158 (Long, 1999; Long et al., 1996).

Found in chromosome 19q13.4, the KIR family consists of 13 genes which are *KIR2DL1*, *KIR2DL2-3*, *KIR2DL4*, *KIR2DL5A*, *KIR2DL5B*, *KIR2DS1*, *KIR2DS2*, *KIR2DS3*, *KIR2DS4*, *KIR2DS5*, *KIR3DL1/DS1*, *KIR3DL2*, and *KIR3DL3*, and also added two pseudogenes; *KIR2DP1* and *KIR3DP1*. Two regions define each KIR hap-

lotype: centromeric (Cen), and telomeric (Tel) regions joined via recombination sites. The four framework genes, *KIR3DL3*, *KIR3DP1*, *KIR2DL4*, and *KIR3DL2*, define the beginning and end of the Cen and Tel regions (Hsu et al., 2002; Martin et al., 2000). Within KIR haplotypes, there are two main groups, A and B. A haplotype has the Cen-A and Tel-A regions and possesses the inhibitory KIR genes, *KIR2DL1*, *KIR2DL2*, *KIR2DL3*, *KIR3DL1*, *KIR3DL2*, *KIR2DL4*, and one activating *KIR2DS4*. The rest of the KIR haplotypes belong to the B group and can carry different Cen-A/B and Tel-A/B combinations. The difference between KIR A haplotypes is determined by allelic polymorphism, while the gene content determines B haplotype difference. This polymorphism is very similar to their ligands, HLA genes. The polymorphism is known to affect the function of these receptors. Such as, *KIR2DL1* A has a higher affinity than *KIR2DL1* B (Pende et al., 2019).

The signaling is determined by the motifs in the cytoplasmic tails, similar to activating signaling. Immunoreceptor tyrosine-based inhibitory motifs (ITIMs) are responsible for counteracting the activating signal from ITAM-mediated signals (Long, 1999). This negative signaling is mediated by the recruitment of tyrosine phosphatases, SHIP, SHP-1, and -2, upon ligand engagement to the receptor and through phosphorylation of ITIMs (Ravetch & Lanier, 2000). The recruited phosphatases start to dephosphorylate the signaling intermediates which have been phosphorylated by the activation signals. This dephosphorylation process results in the termination of cytokine secretion, degranulation, and Ca^{2+} flux, meaning the inhibition of NK cell function. One of the most prominent targets of inhibitory signaling mechanism mediated by inhibitory KIRs is Vav1 by SHP-1-mediated dephosphorylation (Stebbins et al., 2003). Inhibitory KIRs and their HLA ligands are represented in Table 1.

Table 1.1. KIRs and their ligands

KIR	Ligand
2DL1	HLA-C ^{Lys80} (Winter et al., 1998)
2DL2-3	HLA-C ^{Asn80} (Winter et al., 1998)
2DL4	HLA-G (Rajagopalan & Long, 1999)
2DL5	CD155 (Fittje et al., 2022)
3DL1	HLA-Bw4 (Gumperz et al., 1995)
3DL2	HLA-A3, HLA-A11 (Pende et al., 1996)
3DL3	HHLA2 (Bhatt et al., 2021)

KIRs are crucial players in NK cell autoreactivity. NK cell licensing is mediated by KIR expression, in which NK cells that express KIRs for their self-HLA ligands become “licensed”. In the absence of the self-HLA, those NK cells can attack these cells (Anfossi et al., 2006). The ability of educated NK cells to recognize missing-self molecules through a vast KIR repertoire is a field that is being exploited in therapeutic research. The system works in a way that an inhibitory KIR from a donor is given to a patient that lacks the HLA ligand of the given KIR, which in turn results in a “KIR-HLA mismatch” and leads to NK cell cytotoxicity. With KIR-HLA mismatched hematopoietic transplantations, reduced relapse risk and fewer graft rejections were observed (Ruggeri et al., 2002).

1.4. TCR-NK Cells

Genetic modification of T cells to target specific antigens for cancer therapy is a form of adoptive immunotherapy. Amongst the ways of engineering T cells in such a manner to express the specific receptor for the given antigen are TCR-T cells and chimeric antigen receptor (CAR)-T cells (Eshhar & Gross, 1990; Morgan et al., 2006). However, both approaches where targeting is carried through modification on T cells have their restrictions. While CAR-T cells can work in an antigen-dependent manner, they are not HLA restricted; hence, they cannot respond to peptides from intracellular proteins presented on the MHC molecules. This means CARs can only target cell

surface molecules in an antigen-specific manner and targeting intracellular antigens only possible through TCR modification.

However, in the case of TCR-T cells, endogenous TCR expression of T cells can lead to TCR mispairing with the genetically transferred TCR. With the transfer of antigen-specific TCR α and β chains, pairing with endogenous TCR β and α is a risk (Shao et al., 2010). Since there is a chance of autoreactivity due to mispairing, this is a significant problem that needs to be solved. To overcome these challenges, CAR-NK cells have been engineered. They can elicit both T cell and NK cell-mediated responses; however, their lacking in recognition of intracellular antigens drove attention to improve this approach (Shimasaki et al., 2012). To overcome TCR mispairing, several methods have been developed, such as murinization of TCR, where constant domains of TCRs are replaced with murine constant domains, the addition of a second disulfide bond to the TCR's extracellular domain or fused-expression of TCR chains to CD3 ζ (Kuball et al., 2007; Sebestyén et al., 2008; Sommermeyer et al., 2006).

However, another possibility to overcome TCR mispairing is to genetically modify NK cells with engineered TCRs. Since there are no endogenous TCR chains expressed in the NK cell, the mispairing is not a challenge, and NK cells' additional ability to recognize expression loss or downregulation of HLA makes them an excellent candidate. Initially, two studies have shown that these TCR-engineered NK cells can effectively show cytotoxicity against specific antigens by expressing CD3 subunits and TCR chains (Mensali et al., 2019; Parlar et al., 2019). Both studies have shown the functionality and the antigen-specific cytotoxicity of these TCR-engineered NK cells through the expression of either CD3 δ , γ , ϵ and ζ chains (Mensali et al., 2019) or lacking the ζ chain (Parlar et al., 2019). Another recent study has used primary NK cells for this TCR-engineering approach of adoptive immunotherapy. The results showed the enhancement of NK cell cytotoxicity through the addition of TCR-mediated cytolysis (Morton et al., 2022).

The recent TCR-NK studies and some of the other CAR-NK studies rely on the usage of clinically approved, IL-2-dependent NK cell line, NK-92, isolated from a 50-

year-old patient with non-Hodgkin's lymphoma. These cells are highly cytotoxic with surface expression of CD56^{bright} and negative for CD16. They lack most inhibitory KIRs except KIR2DL4 (Maki et al., 2001).

Although a novel adoptive immunotherapy approach, TCR-NK cell therapy has shown promising results. But the limitations of using a clinical grade NK cell line for the expression of TCR chains in inhibitory receptor expression are unignorable. While the recent primary TCR-NK approach has given a glimpse of the NK cell-mediated cytotoxicity in the absence of HLA expression, further characterization and investigation of the different inhibitory signals with TCR signaling must be uncovered.

2. AIM

While the TCR-NK approach is promising for targeting intracellular antigens using NK cells, it is yet unclear how the inhibitory signaling in NK cells would interact with the TCR signals and whether this interaction would render KIR-expressing NK cells dysfunctional in terms of TCR-mediated triggering. This study aimed to investigate the possible links and effects of inhibitory signals relayed from inhibitory KIR2DL1 receptor and the present TCR signaling in NK-92 cells expressing a functional TCR-CD3 complex on their surface against the melanoma-associated antigen tyrosinase. With this primary approach, this study specifically aims:

- To express a functional KIR2DL1 protein NK-92 cells with functional TCR-CD3 complex through genetic modification.
- To assess the function of KIR2DL1 expression on the antigen-specific cytotoxicity of TCR-NK cells.

3. MATERIALS AND METHODS

3.1. Materials

3.1.1. Chemicals

Chemicals used in this study are provided in Appendix A.

3.1.2. Equipment

Equipments used in this study are provided in Appendix B.

3.1.3. Buffers and Solutions

Calcium Chloride (CaCl₂) Solution: 60 mM CaCl₂ (from 1M stock), 15% autoclaved glycerol and 10 mM PIPES (pH 7.00) were mixed at 250 ml final volume completed by ddH₂O and sterilized by filtering with 0.22 µm filter.

Agarose Gel: For 100 ml 1% w/v gel, 1 g of agarose powder was dissolved in 100 ml 0.5X TBE by heating, then 0.01% v/v ethidium bromide was added.

Tris-Boric Acid-EDTA (TBE) Buffer: To obtain 5X 1L stock solution 54 g tris-base, 27.5 g boric acid and 20 ml 0.5M EDTA (pH 8.00) were mixed in 1 L of ddH₂O. For 0.5X working solution, the stock was diluted 1:10 with ddH₂O, and stored at room temperature.

HBS solution (2X): 280 mM NaCl, 50 mM HEPES, and 1.5 mM Na₂HPO₄ were mixed at 200 ml final volume with ddH₂O, and pH is adjusted to 7.00-7.10 with 10 M NaOH. Sterilization was done with 0.22 µm filter. Stored at -20°C.

PEG8000 50%: For 1 liter of 50% w/v, 500 gr PEG8000 was dissolved in 1 L ddH₂O. Sterilized by autoclave, and stored at room temperature.

Running Buffer (10X): For 1 liter of 10X running buffer, 144.1 g glycine, 30.3 g tris-base and 10 g SDS was dissolved in 1 liter of ddH₂O. For 1X working solution, solution was diluted at 1:10 with ddH₂O, and stored at room temperature.

Wet Transfer Buffer (10X): For 1 liter of 10X wet transfer buffer, 144.1 g glycine and 30.3 g tris-base was dissolved in 1 liter of ddH₂O. For 1X working solution, 200 ml methanol, 100 ml 10X buffer, and 700 ml ddH₂O was mixed, and stored at 4°C.

TBS and TBS-T: For 10X TBS 88 g NaCl and 24 g tris-base was dissolved in 1 L dH₂O and pH was adjusted to 7.6. 1X TBS was prepared by diluting this solution to 1:10 with ddH₂O. Additionally, 1X TBS-T was prepared by adding 1 ml of Tween in 1 L 1X TBS.

3.1.4. Growth Media

Luria Broth (LB): For 1X LB media, 20 g LB powder was dissolved in 1 L ddH₂O, and autoclaved at 121°C for 20 minutes.

LB Agar: 16 g LB powder and 12 g bacterial agar powder were diluted in 800 ml ddH₂O and autoclaved at 121°C for 15 minutes to make a 1X agar medium. Then, poured into sterile Petri dishes after addition of the desired antibiotic. After plates are cooled down, they were stored at 4°C.

Complete DMEM: HEK293FT cells were maintained in 10% heat-inactivated FBS supplemented DMEM with 0.1 mM MEM non-essential aminoacid solution, 25 mM HEPES, 1 mM sodium pyruvate and 2 mM L-Glutamine.

Complete RPMI 1640: RPMI 1640 medium is supplemented with 20% heat inactivated FBS, 0.1 mM MEM non-essential aminoacid solution, 25 mM HEPES, 1

mM sodium pyruvate, 2 mM L-Glutamine, 1X MEM vitamin, and 0.1 mM 2 mercaptoethanol for the maintenance of NK-92 cells.

Freezing Medium: All the cells were frozen in 6% DMSO in heat inactivated FBS (v/v).

3.1.5. Commercial Kits

Table 3.1. List of commercial kits

Commercial Kit	Company
NucleoBond® Xtra Midi EF	Macherey-Nagel, USA
NucleoSpin® Gel and PCR Clean-up	Macherey-Nagel, USA
NucleoSpin® Plasmid	Macherey-Nagel, USA

3.1.6. Enzymes

Table 3.2. List of enzymes

Enzymes	Company
ApaI	New England Biolabs, USA
BamHI-HF	New England Biolabs, USA
BsaI	New England Biolabs, USA
CIAP	New England Biolabs, USA
EcoRI-HF	New England Biolabs, USA
NdeI	New England Biolabs, USA
Q5 Polymerase-HF	New England Biolabs, USA
T4 Ligase	New England Biolabs, USA
Taq Polymerase	Thermo Fischer, USA
XhoI	New England Biolabs, USA

3.1.7. Antibodies

Table 3.3. List of antibodies

Antibodies	Company
Anti-CD56 PE-conjugated	BD BioSciences
Anti-CD107a APC-conjugated	BD BioSciences
Anti-KIR2DL1 APC-conjugated	BD BioSciences
Anti-CD3 ϵ APC-conjugated	BD BioSciences
Anti-TCR $\alpha\beta$ APC-conjugated	BD BioSciences
Anti-TNF- α APC-conjugated	BD BioSciences
Anti-IFN- γ APC-conjugated	BD BioSciences

3.1.8. Bacterial Strains

Escherichia coli (*E. coli*) Top10 strain is used for all plasmid amplifications including lentiviral constructs' amplifications.

3.1.9. Mammalian Cell Lines

HEK293FT: Fast-growing, highly transfectable human embryonic kidney cells that transformed with SV40 large T antigen (Invitrogen R70007).

NK-92: Human natural killer cell line, isolated from a 50-year old patient with non-Hodgkin's lymphoma (ATCC® CRL 2407™)

K562: Lymphoblast cells isolated from a 53-year old patient with a chronic myelogenous leukemia (ATCC® CCL-243™).

A375 and A375-Tyr: Malignant melanoma cells isolated from a 54-year old patient's skin (ATCC® CRL-1619™) and its tyrosinase gene overexpressing version.

3.1.10. Plasmids and Oligonucleotides

Table 3.4. List of plasmids

Plasmids	Purpose	Source
LeGO-DGE-IRESpuro	Lentiviral construct for expression of CD3 subunits: δ , γ , and ϵ	Lab construct
LeGO-DGEZ-IRESpuro	Lentiviral construct for expression of CD3 subunits: δ , γ , ϵ , and ζ	Lab construct
TyrTCR-IRES-eGFP (TyrTCR)	Lentiviral construct for expression of TCR α and β chains specific for tyrosinase	Gift from Brusko et al.
LeGO-KIR2DL1-iT2	Lentiviral construct for KIR2DL1 expression with IRES and tdTomato	Lab construct
pMDLg/pRRE	Virus production/packaging plasmid (Gag/Pol)	Addgene (#12251)
pRSV-REV	Virus production/packaging plasmid (Rev)	Addgene (#12253)
pCMV-VSV-g	Virus production/packaging plasmid (Env)	Addgene (#8454)

Table 3.5. List of oligonucleotides

Oligo Name	Sequence (5' to 3')	Purpose
IRES_seqF	TTAAAAAACGTCTAGGCC	Confirmation of LeGO-DGE-IRES _{puro} vectors
WPRE_R	CATAGC GTAAAAGGAGCAACA	Confirmation of LeGO-DGE-IRES _{puro} vectors

3.2. Methods

3.2.1. Bacterial Cell Culture

Bacterial culture growth: The following growth procedure was performed for every bacterial culture. Top10 *E. coli* cells were cultured in 1X LB media supplemented with ampicillin at 37°C for overnight (16 hours) at 220 rpm shaking incubator. Then, cells were spread on LB agar plates (ampicillin) with glass beads, and incubated overnight at 37°C. Later, single colonies were picked. To obtain glycerol stocks, the chosen single colony was grown in 3 ml LB medium at 37°C overnight, shaken at 220 rpm and followed by 1:3 dilution with fresh LB medium and cultured at 37°C shaker incubator at 220 rpm for 6 hours. When bacterial cells were at their logarithmic phase of their growth curve, they were mixed with glycerol of final concentration of 10% (v/v) in 1 ml, and stored at -80°C.

Competent Bacteria Preparation: From glycerol stock of Top10 *E. coli*, a 3 ml culture was started at 37°C, with shaken incubator at 220 rpm for 6 hours. Then, the culture was transferred to 50 ml LB and incubated at 220 rpm, 37°C for overnight. Next day, 4 ml of the overnight culture was diluted into 400 ml of LB in 2 L flask. Incubation lasted until the OD₅₉₀ is 0.375. After that, 400 ml culture was divided into eight 50 ml tubes and incubated on ice for 10 minutes. Then, cells were centrifuged at 1600 *xg* for 10 minutes, at 4°C (all the centrifugation steps performed at 4°C). After

the supernatant is discarded, pellets were resuspended in 10 ml ice-cold CaCl_2 and centrifuged at 1100 xg for 5 minutes. Again, supernatant was discarded and pellets were resuspend in 2 ml CaCl_2 and incubated on ice for 30 minutes. After incubation, the tubes were mixed in one tube then aliquoted as 100 μl in tubes and snap-frozen with liquid nitrogen, and stored at -80°C .

Transformation of Competent Bacteria: During every transformation both plasmid DNA and competent bacterial cells were thawed on ice. Transformation is performed as following: plasmid DNA was added to competent cells and incubated on ice for 30 minutes. After that, at 42°C for 90 seconds, cells were heated followed by heat-shock on ice for 1 minute. Then, to each competent cell-plasmid DNA mix, 900 μl LB was added and incubated at 37°C for 45 minutes. After incubation, cells were centrifuged at 13,000 rpm for 1 minute. 900 μl of supernatant was discarded and the cells were resuspended in the remaining 100 μl . Then, cells were spread on appropriate antibiotic containing LB agar plates by glass beads and left for incubation at 37°C for overnight.

Plasmid DNA Isolation: For both mini- and midi-culture, Macherey-Nagel NucleoSpin® Plasmid or NucleoBond® Xtra Midi EF kits were used according to manufacturer's protocols, respectively. Final DNA concentration and purity were measured by NanoDrop spectrophotometer.

3.2.2. Mammalian Cell Culture

Maintenance of Cell Lines: HEK293FT cells were maintained in complete DMEM. When cells reached an 80% confluency, they were first washed with DPBS to remove residual FBS. Then, 0.025 Trypsin-EDTA was used to dissociate cells at 37°C , for 5 minutes. After resuspension of cells with the complete DMEM, cells were re-seeded at a 1:5 ratio for two days. For NK-92 cells, cells were maintained at 350,000 cell/ml with fresh 1000 IU/ml IL-2 every two days in complete 20%FBS RPMI-1640 media. K562 cells were kept at 200,000 cell/ml for every two days in 10%FBS RPMI-1640 media. A375 and A375Tyr cells were split at 80% confluency every two or three days

by first a DPBS wash followed by trypsinization with 0.025 Trypsin-EDTA. Cells were resuspended with 10% FBS RPMI-1640 media and seeded at 1:10 ratio for two days.

Cell Freezing: For NK92 cells, prior to the freezing day, cells were set to 500.000 cells/ml for minimum of 5×10^6 cell. Next day, cells were counted again and for each vial the final volume was set to 1 ml of 6% DMSO in FBS. Cells were collected and centrifuged to remove the culture media. Half of the total volume was given to cells as full FBS, and cells were incubated at 4°C for 20 minutes. Rest of the volume was prepared as 12% DMSO in FBS. After incubation cell-FBS and DMSO-FBS solutions were mixed and the vials were kept in a Mr. Frosty for at least 24 hours at -80°C, then stored at -80°C.

Cell Thawing: All cell lines were thawed within 5 ml FBS, followed by centrifugation at 300 *xg* for 5 minutes. The cell pellet was resuspended in their respective cell culture media. All cell lines were incubated at 37°C, 5% CO₂.

3.2.3. Design and Cloning

In this study, to obtain puromycin-resistant expression of three CD3 subunits, the existing LeGO-DGE-IRES-TCR backbone was used where TCR fragment is replaced by puromycin resistance gene (puro-insert) obtained from LeGOiG2p vector with PCR.

PCR for Puro-insert from LeGOiG2p: To obtain puro-insert from the backbone with desired restriction enzyme sites which were EcoRI and XhoI.

PCR for Puromycin Insert:

LeGOiG2p	2.5 ng
5X Q5 Reaction Buffer	10 μ l
dNTP	1 μ l
10 μ M puro_ext_EcoRI_fwd	2.5 μ l
10 μ M puro_ext_XhoI_rev	2.5 μ l
GC Enhancer	10 μ l
NEB Q5 High-Fidelity	0.5 μ l
ddH ₂ O	up to 50 μ l
Total volume	50 μ l

PCR Conditions:

Step	Temperature	Time
Initial denaturation	98°C	30 seconds
30 Cycles	98°C	10 seconds
	62°C	30 seconds
	72°C	21 seconds
	72°C	21 seconds
Final Extension	72°C	2 minutes

After the PCR is completed, the PCR product was run on 0.7% agarose gel prepared with TBE for 1 hour at 100 V. For the isolation of PCR product, NucleoSpin® Gel and PCR Clean-up kit was used according to manufacturer's protocol. Eluted DNA concentration was measured with NanoDrop spectrophotometer.

Digestion of Puromycin Insert and LeGO-DGE-IRES-TCR Backbone:

Eluted insert and the backbone were digested using EcoRI and XhoI by following the below reaction;

Digestion of LeGO-DGE-IRES-TCR:

LeGO-DGE-IRES-TCR	10 µg
NEB XhoI (10,000 IU/ml)	1.5 µl
NEB EcoRI-HF (10,000 IU/ml)	1 µl
NEB CutSmart Bufferd	5 µl
ddH ₂ O	up to 50 µl
Total volume	50 µl

Digestion of Puro-insert:

PCR product for puromycin	1.5 µg
NEB XhoI (10,000 IU/ml)	0.75 µl
NEB EcoRI-HF (10,000 IU/ml)	0.5 µl
NEB CutSmart Bufferd	5 µl
ddH ₂ O	up to 50 µl
Total volume	50 µl

Digestion reactions were carried out at 37 °C for 2 hours. To remove the extracted fragment from LeGO-DGEiTCR, reaction was run on 0.7% agarose gel made with TBE, for 1 hour at 100 V. NucleoSpin® Gel and PCR Clean-up kit was used according to manufacturer's protocol. Eluted DNA concentration was measured with NanoDrop spectrophotometer.

Eluted backbone was treated with calf intestinal alkaline phosphatase (CIP) to dephosphorylate 5' and 3' DNA ends to prevent self-ligation of the backbone.

CIP Treatment of the Backbone:

Extracted LeGO-DGE-IRES-TCR (300 ng of the product was reserved for ligation control)	34 μ l
NEB CIP (10,000 IU/ml)	0.1 μ l
NEB CutSmart Bufferd	5 μ l
ddH ₂ O	up to 50 μ l
Total volume	50 μ l

CIP reaction is carried out at 37°C for 30 minutes. Following the incubation, the product was eluted by NucleoSpin® Gel and PCR Clean-up kit. Ligation of the insert and backbone carried out at 16°C for 16 hours, as described below:

Digested puro-insert	3.5-17 ng
CIP-treated LeGO-DGE-IRES-TCR	50 ng
NEB T4 DNA Ligase	1 μ l
NEB 10X T4 DNA Ligase Buffer	2 μ l
ddH ₂ O	up to 20 μ l
Total volume	20 μ l

Transformation of the Ligation Reaction and Confirmation of the Cloning: 10 μ l of the ligation reaction was transformed into 100 μ l competent E. coli cells. Next day colonies were picked for colony PCR. Mini-cultures' of positive colonies were prepared and control digestions were performed to determine the correct colonies.

First conformation of the cloning was performed with colony PCR. The reaction was carried out as following:

Colony	pick
10X Taq Buffer	2.5 μ l
25 mM MgCl ₂	1.5 μ l
10 mM dNTP	0.5 μ l
10 μ M IRES_seqF	0.5 μ l
10 μ M WPRE_rev	0.5 μ l
Taq polymerase	0.125 μ l
ddH ₂ O	up to 25 μ l
Total volume	25 μ l

PCR Conditions:

Step	Temperature	Time
Initial denaturation	95°C	3 minutes
30 Cycles	95°C	30 seconds
	48°C	30 seconds
	72°C	54 seconds
	72°C	54 seconds
Final Extension	72°C	5 minutes

After completion PCR, the samples were run on a 1% 0.5X TBE at 100 V. Two positive colonies were picked to start mini cultures, and isolated with Macherey-Nagel NucleoSpin® Plasmid kit according to manufacturer's protocols.

3.2.4. Lentiviral Particle Production

For the production of lentiviral infectious particles, HEK293FT cells were transfected accordingly: 16 hours prior to transfection, 4.5x10⁶ HEK293FT cells were seeded in 100 mm culture dishes. Then, 7.5 μ g gene-of-interest, 3.75 μ g pMDLg/pRRE, 2.5 μ g pRSV-REV, and 1.25 μ g pHCMV-VSV-G plasmids were co-transfected with the cal-

cium phosphate precipitation method where plasmids were mixed with 50 μ l of CaCl_2 and completed to 500 μ l with ddH₂O. Then, the DNA- CaCl_2 mix was added to 500 μ l 2X HBS drop by drop. After 15 minutes of incubation, the mixture was added to cells in the presence of 25 μ M chloroquine. 8 hours later the medium was changed, and virus supernatant was collected at 48-hour time point and filtered through a 0.45 μ m filter and directly PEGylated at final 10% PEG, and left at 4°C overnight. After overnight incubation, virus-PEG solution was centrifuged at 3000 xg for 30 minutes. Supernatant was discarded, and remaining PEG-coated viral particles were resuspended in appropriate amount of serum-free RPMI-1640, and stored at -80°C.

3.2.5. Lentiviral Transduction of NK-92 Cells

To obtain stable expression of each gene of interest, NK92 cell line of to be transduced was set to 500.000 cell/ml prior to transduction day. At transduction day, cells were transduced with the chosen infectious particle at MOI=5 where cell line was kept at 1×10^6 cells, as duplicates. Transduction was performed under 1.5 μ M (5Z)-7-Oxozeaenol, 8 mg/ml protamine sulfate, and 1000 IU IL-2. After 16 hours, virus-containing media was replaced with fresh media. Before the control of the gene expression, cells were maintained in this medium for three or four days. For both CD3 and KIR2DL1 modifications, gene expression was controlled by flow cytometry.

3.2.6. Flow Cytometry

In this study, all the flow cytometry assays were carried out as follows. Surface stainings were performed by first washing the cells with DPBS followed by appropriate amount of antibody on ice for 30 minutes. After incubation, cells were washed with DPBS again to remove residual antibody, and analysis was performed. For surface stainings 2×10^5 cells were used. KIR2DL1 positive cells were sorted in 1.5% FBS-DPBS, followed by incubation in 20% FBS complete RPMI-1640 media supplemented with 1% Penicillin-Streptomycin. Cells were acquired with BD Accuri C6 and BD FACsCalibur, sorted with BD Influx and analyzed with FlowJo software.

3.2.7. Degranulation of TCR-NK Cells

Prior to experiment, effector cells and one of the target cell K562 were seeded at 500,000 cell/ml, while A375 and A375Tyr was seeded at the experiment day. Next day, all cells were recounted and adjusted to 200,000 cell per 100 μ l for every well of the v-bottom 96-well plate. Prior to seeding on 96-well plate, incubation of effector NK cells with anti-CD107a-APC-conjugated was started. As positive control, phorbol 12-myristate 13-acetate (PMA) and ionomycin were used on effector cells at 1.25 μ g/ml and 0.25 μ g/ml final concentrations respectively. Then, cells were centrifuged at 50 *xg* for 2 minutes. Effector and target cells were incubated at a 1:1 ratio for 1 hour at 37°C, 5% CO₂ incubator. After incubation, monensin was added to each well and, centrifuged at 50 *xg* for 2 minutes prior to further incubated for 3 hours. At the end of total of 4 hours, plate was centrifuged at 400 *xg* for 5 minutes. Supernatant was discarded and WT NK cells were stained with CD56 PE-conjugated antibody at 1:50 ratio for 30 minutes on ice. Remaining samples are transferred to FACS tubes and analysis was performed. For time-point degranulation, 15', 30', 45' and 60' time-points did not include monensin treatment, but directly analyzed.

3.2.8. Real-time Cell Analysis of TCR-NK Cells

Prior to experiment day, effector cells were seeded at 500,000 cells/ml. The same day, target cells were plated on E-16 plates in the following manner: Each E-16 plate to be used was first incubated at room temperature with 200 μ l target medium for 15 minutes. Following the incubation, a background reading was performed on the xCelligence device. Then, 100 μ l of the medium was removed and 10,000 cells/well target cell was seeded into appropriate wells. After 16 hours, 100 μ l of the medium was removed and appropriate amounts of effector cells were seeded in each well with 1000 IU IL-2 was given into each well. Cell index was measured for the following 24 hours.

3.2.9. Intracellular TNF- α and IFN- γ Staining

Similar to degranulation analysis, effector cells and target cells were seeded at 500,000 cell/ml prior to experiment day, with the exception of A375 and A375Tyr. Next day, cells were co-incubated at 1:1 ratio with 200,000 effector cells. As opposed to degranulation, CD107a staining was not performed. After 1 hour of co-incubation Brefeldin-A was added. Completion of the total 4 hours, for intracellular staining, cells were fixed and permeabilized with 1% PFA and 0.01% w/v Saponin in DPBS for 30 minutes. After washing cells with permeabilization wash buffer two times. Cells were analysed in a flow cytometer.

3.2.10. Statistical Analysis

All statistical analysis was performed using GraphPad Prism 9.0.0 and two-way ANOVA test was used to determine the significance.

4. RESULTS

4.1. Cloning of CD3 and Receptor Vectors

4.1.1. Cloning of LeGO-DGE-IRES-puro

As described in Methods, following the ligation, colony PCR was performed with the picked colonies using IRES_seqF and WPRE_rev primers. The expected band size for the positive colonies was 890 bp, while for the intact vector the band size was 2123 bp (Figure 4.1a). As seen in Figure 4.1b, 4th and 10th colonies have given the right bands.

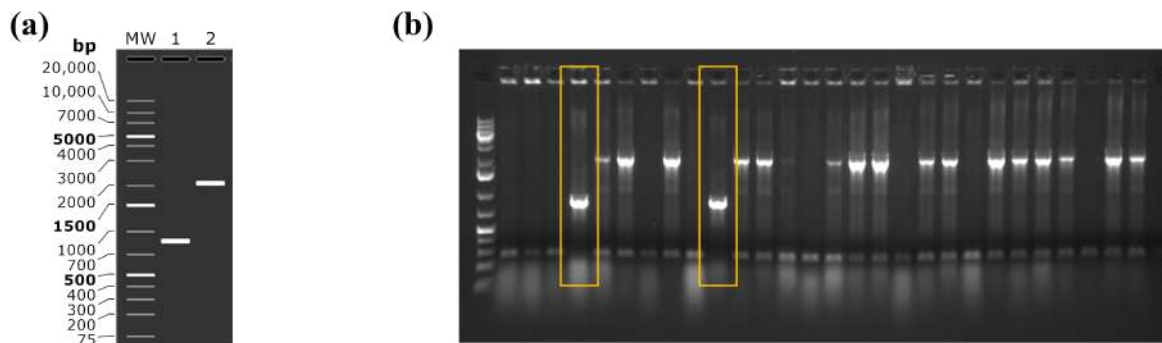


Figure 4.1. Gel images of predicted and actual colony PCR results of LeGO-DGE-IRESpuro.

(a) MW indicates the DNA ladder, 1st well representing the successfully cloned LeGO-DGE-IRESpuro's expected band and 2nd well representing the empty vector's band. (b) Wells marked with yellow rectangles represent the positive colonies.

Selected colonies were isolated from their mini-cultures and restriction digestion with EcoRI and XhoI, and BamHI as shown in Figure 4.2.

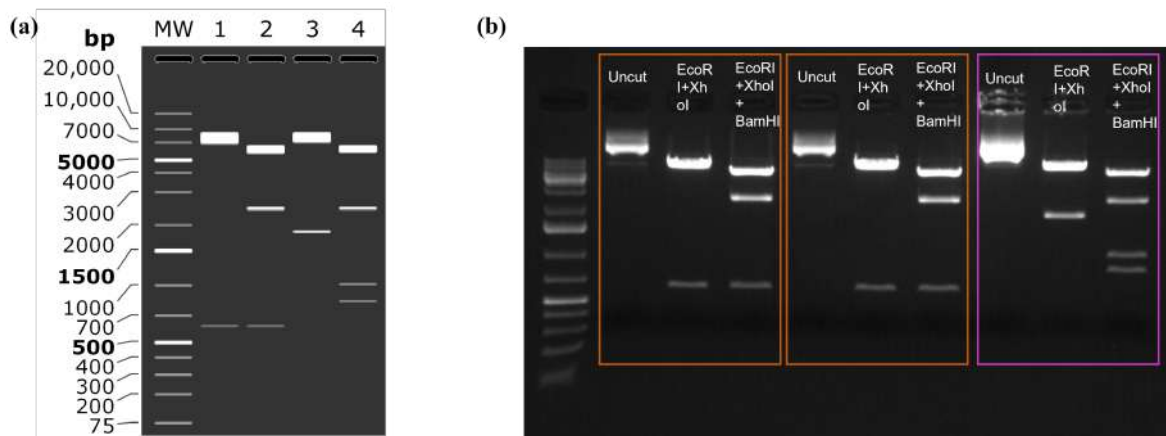


Figure 4.2. Gel images of predicted and actual restriction digestion results of LeGO-DGE-IRESpuro vectors

(a) MW indicates the DNA ladder, 1st well representing the successfully cloned LeGO-DGE-IRESpuro's expected bands when digested with EcoRI and XhoI, 2nd well representing the expected bands when digested with EcoRI, XhoI, and BamHI. 3rd well represents the expected bands of the backbone vector, LeGO-DGEiTCR after digested with EcoRI and XhoI, while the 4th well represents the digestion after EcoRI, XhoI, and BamHI. (b) Orange brackets represents the colonies picked from the colony PCR results, and their digestion with the annotated enzymes, while the purple brackets show the backbone vector, LeGO-DGEiTCR digestion.

After the two positive colonies were selected following colony PCR and restriction digestion controls, vectors were final tested in transfection by co-transfecting HEK293FT cells with the TyrTCR-GFP vector to determine the surface CD3 expression levels.

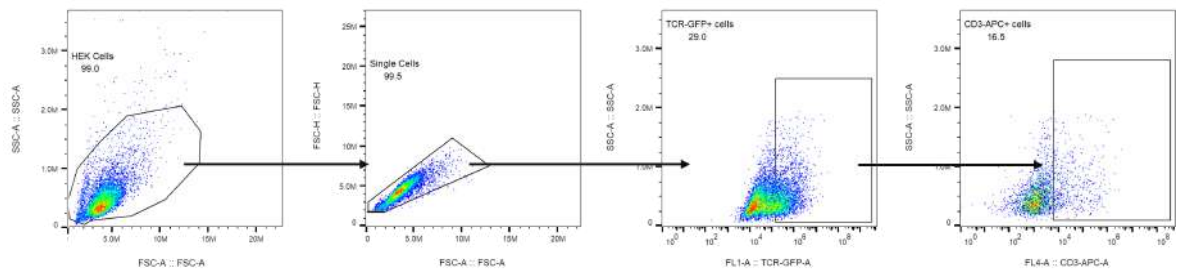


Figure 4.3. Flow cytometry analysis of CD3 ϵ surface expression on 293FT cells, co-transfected with TCR $\alpha\beta$ chains.

In Figure 4.3, the gating strategy is as follows; after HEK293FT cells were selected, single cells were gated at FSC-A vs FSC-H. From single cells, GFP positive cells, which the signal came from TCR chains were selected and CD3 ϵ expression was detected via anti-CD3 ϵ APC-conjugated antibody.

4.1.2. Confirmation of LeGO-KIR2DL1-iT2

Lab constructs of LeGO-KIR2DL1-iT2 vector was confirmed using two different enzymatic reaction combinations using XhoI and BsaI, and ApaI and NdeI, represented in Figure 4.4.

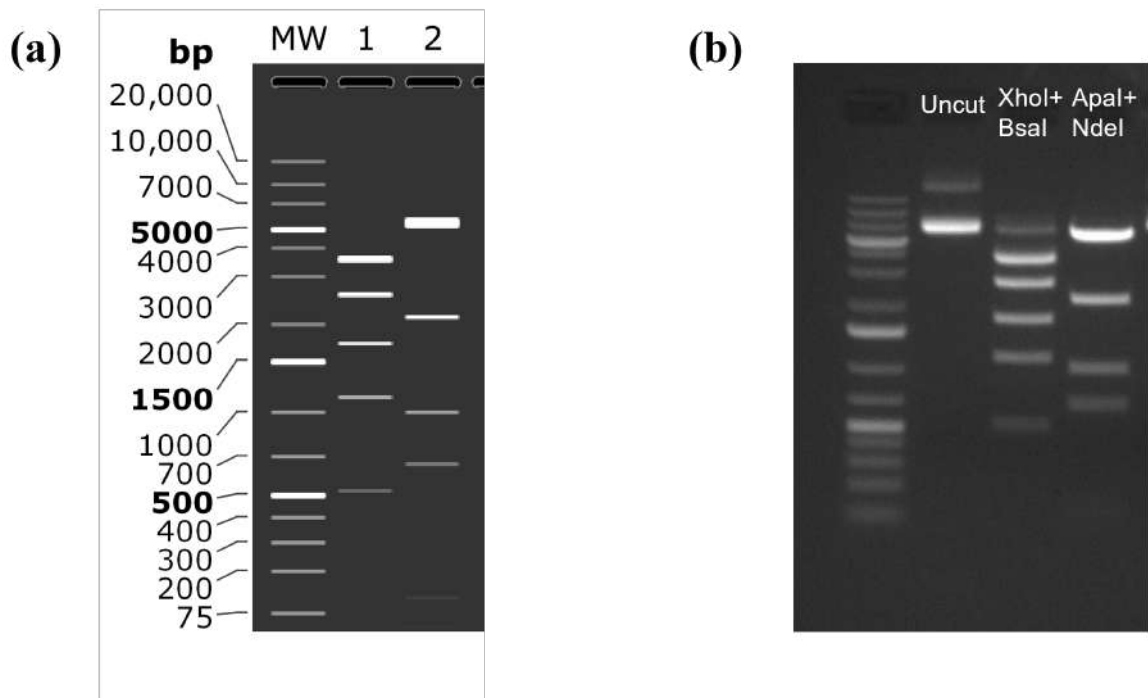


Figure 4.4. Gel images of predicted and actual control digestion results of LeGO-KIR2DL1-iT2

(a) MW indicates the DNA ladder, 1st well representing the successfully cloned LeGO-KIR2DL1-iT2's expected bands with XhoI and BsaI double digestion, and 2nd well representing bands for ApaI and NdeI double digestion. (b) LeGO-KIR2DL1-iT2 digestions under annotated enzymatic conditions.

Colony that has been confirmed by both colony PCR and control digestion was used for further KIR2DL1 lentiviral construct productions.

4.2. Lentiviral Vector Productions

For the generation of stable expression of TCR complex and KIR2DL1 on NK92 cells, 2 lentiviral constructs were used (Figure 4.5). VSV-G pseudotyped lentivirus production was generated by transfecting HEK293FT cells.

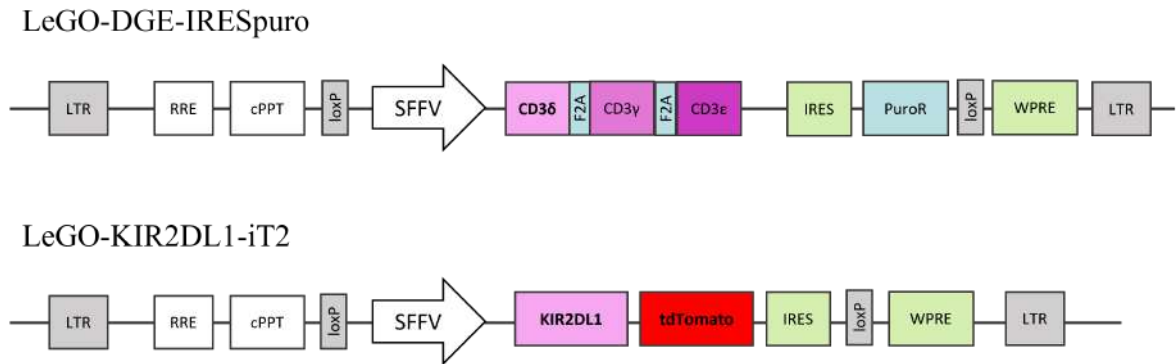


Figure 4.5. Lentiviral constructs for CD3 subunits and KIR2DL1.

Viral titers were determined by transducing HEK293FT cells with different dilutions of the viral particles. Titrations were shown in Table 4.1.

Table 4.1. Table of viral titers

Lentivirus	Collection Time	Infectious particle per ml
LeGO-DGE-IRESpuro	48 hours	1.83×10^6
LeGO-KIR2DL1-iT2 (PEGylated)	48 hours	2.8×10^6

4.3. Genetic Modification of NK92-TyrTCR Cells

In this study, NK-92 cells were transduced with lentiviral particles overnight in the presence of (5Z)-7-Oxozeaenol and protamine sulphate, and gene expression analysis were carried out by flow cytometry. After 4 days, either puromycin selection was started, or cells were expanded to be sorted by FACS.

4.3.1. Genetic Modification of NK-92-TCR Cells with CD3 Subunits

For the expression of a functional TCR-CD3 complex on the NK-92 cell surface, lentiviral particles obtained from HEK293FT cell transfection of CD3 subunits were

used. Lentiviral transduction was performed on stable NK-92 cells that were priorly transduced and FACS sorted with TyrTCR-GFP expression.

In Figure 4.6, CD3 ϵ expression before and after puromycin selection was observed by flow cytometry.

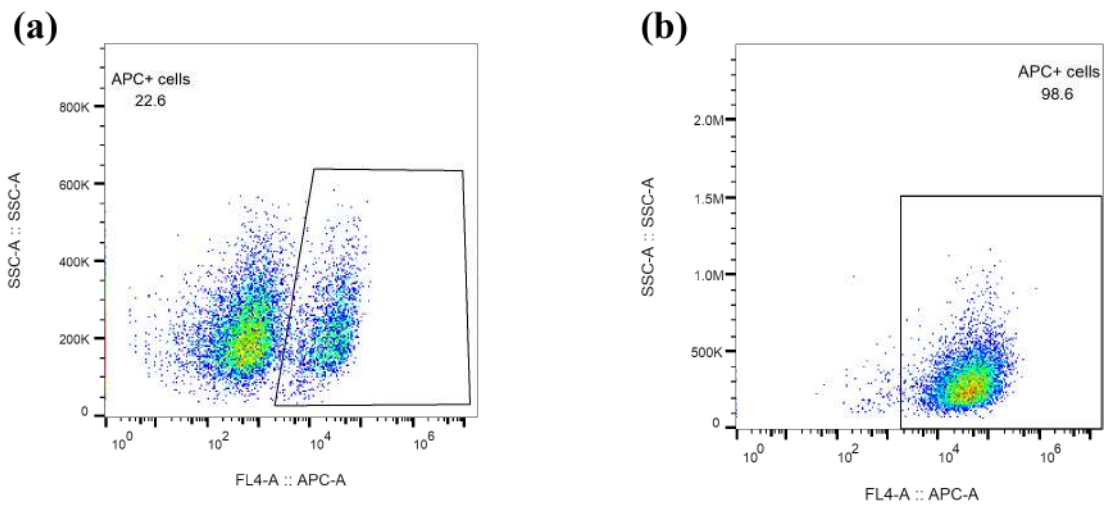


Figure 4.6. Flow cytometry results of transduction of NK-92TCR cells with CD3 subunits, followed by puromycin selection.

(a) surface CD3 ϵ expression before puromycin selection, and (b) after puromycin selection.

Puromycin selection of 4 days resulted with a CD3 surface expression increase from 22.6% to 98.6%, proving a successful selection. Obtained cell line was used for transduction of KIR2DL1 later, and called NK-92TCR(DGE) from this point.

4.4. Genetic Modification of NK-92TCR(DGE) Cells with KIR2DL1

4.4.1. FACS Sorting of KIR2DL1 Expressing NK-92TCR(DGE) Cells and Surface Analysis

KIR2DL1 containing lentiviral particles was used to transduce NK-92TCR(DGE) cells to achieve stable KIR2DL1 expression.

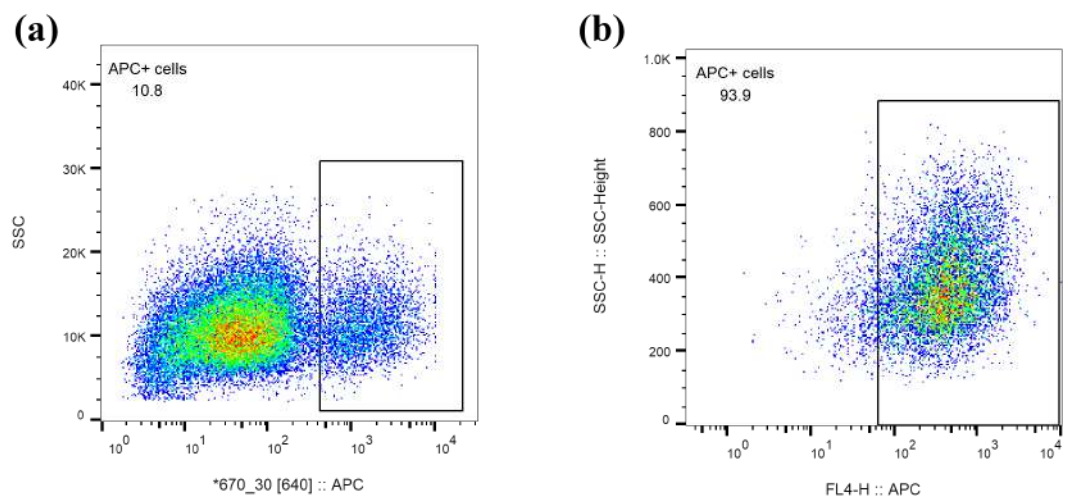


Figure 4.7. KIR2DL1 surface expression of NK-92TCR(DGE) cells assessed by flow cytometry.

(a) Before and (b) after FACS sorting according to KIR2DL1 expression.

A population of 10.8% KIR2DL1 expressing NK-92TCR(DGE) cells was sorted (Figure 4.7a) to obtain a cell line which was called NK-92TCR(DGE)-KIR2DL1. Following the sort, cells were again stained with the same antibody used for sorting to observe the final KIR2DL1 surface expression. As can be seen in Figure 4.7b, 93.9% of KIR2DL1 surface expression was obtained.

4.5. Functionality of TCR-NK KIR2DL1 Cells

Evaluation of the effect and function of KIR2DL1 expressing cells were measured by assays that were common in NK cell cytotoxicity measurements. These are, degranulation, cytotoxicity, and cytokine secretion. Also, the assessment of the downstream molecular effect of the inhibitory signal on the intermediates between TCR and NK signaling was measured with Western blot analysis on phosphorylated proteins.

4.5.1. Degranulation of Antigen-specific TCR-NK KIR2DL1 Cells

NK cell triggering results with release of cytolytic granules such as perforin and granzyme B through lysosomes. During degranulation, CD107a molecules inside the lysosomal membrane comes to surface and the surface expression levels of CD107a was used to determine the NK cell degranulation. The assays were set as explained in Materials and Methods.

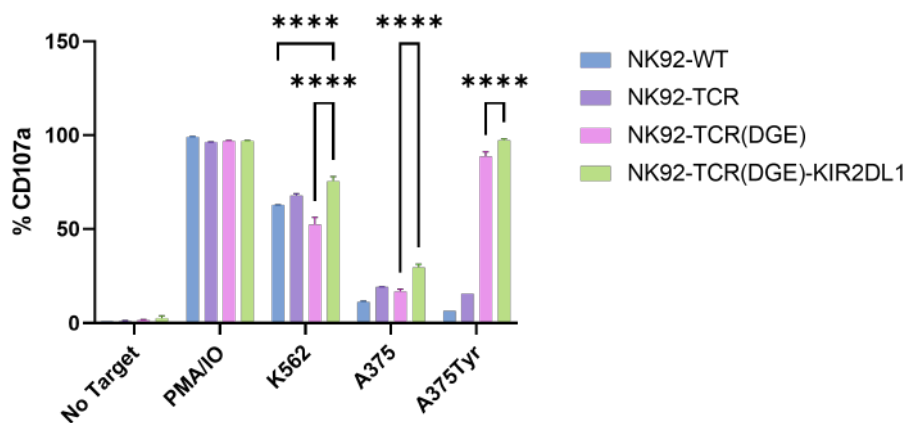


Figure 4.8. Degranulation of NK-92TCR(DGE)-KIR2DL1 cells.

Degranulation of effector cells was measured by surface CD107a levels. At an effector:target 1:1 ratio, all effector cells were stimulated with PMA/IO, and K562.

For antigen-specific cytotoxicity, CD107a levels of each effector against A375 and

A375Tyr cells. (Two-way ANOVA analysis, **** $p < 0.0001$)

The first degranulation assay results showed the co-incubation of effectors and targets for 4 hours. From Figure 4.8, surface CD107a levels of NK-92TCR(DGE)-KIR2DL1 cells were significantly higher against NK-92TCR(DGE) control cells against all targets except PMA/IO simulation. Further analysis of degranulation profile of the KIR2DL1 expressing effector cells were measured at different time points.

Whether the effect of inhibitory signal shows a difference at early time points, another degranulation assay was set where co-incubation was terminated at 1 hour.

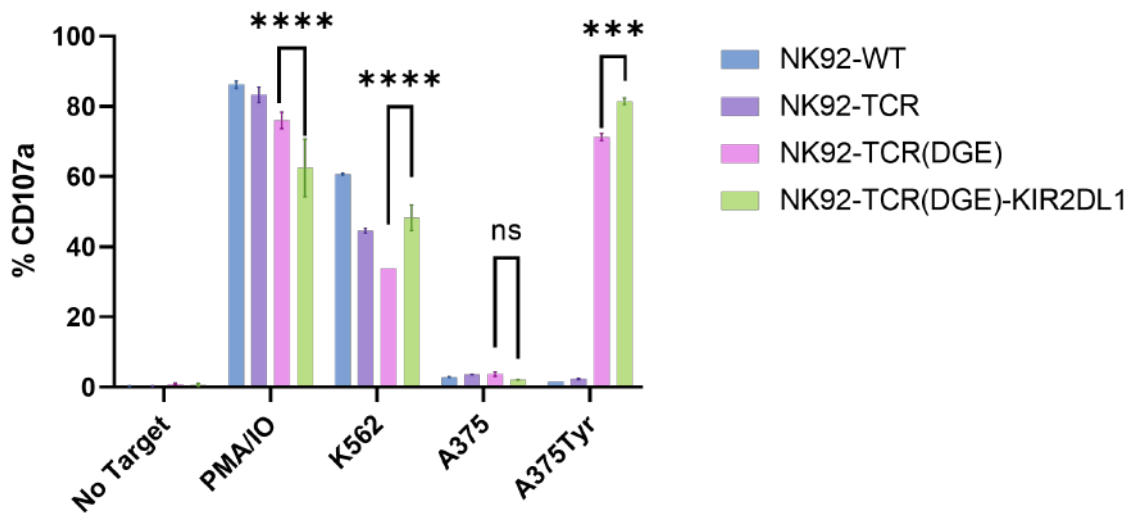


Figure 4.9. Degranulation of NK-92TCR(DGE)-KIR2DL1 cells for 1 hour.

Degranulation of effector cells was measured by surface CD107a levels. At an effector:target 1:1 ratio, all effector cells were stimulated with PMA/IO, and K562. For antigen-specific cytotoxicity, CD107a levels of each effector against A375 and A375Tyr cells (Two-way ANOVA analysis, **** $p < 0.0001$, *** $p = 0.0008$, ns= not significant).

The 1-hour co-incubation of effectors with their targets showed a similar result with 4 hours assay. Again, KIR2DL1 expressing effector cells have shown higher CD107a levels against K562 and A375Tyr. However, a significant decrease against PMA/IO stimulation was observed in KIR2DL1 expressing cells against control cells, and no significance was observed against A375 cells (Figure 4.9).

To assess the dynamics of degranulation that can be affected by inhibitory signals, a time-point degranulation assay was performed in which effector and target co-incubations were terminated at 15, 30, 45, 60, 90, and 120 minutes.

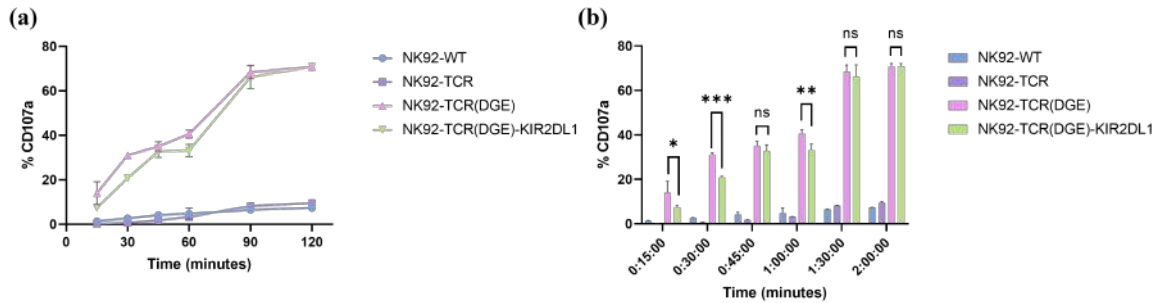


Figure 4.10. Degranulation of KIR2DL1 expressing cells against A375Tyr cells at different time points.

(a) line and (b) bar representation of the time-point degranulation assay. At early time-points KIR2DL1 expressing cells showed a significant decrease, however later the difference was not significant (Two-way ANOVA analysis. * $p=0.0196$, ** $p=0.0067$, *** $p=0.0002$).

The significant increase observed in 4-hour degranulation assay against A375Tyr cells was not observed at early timepoints of degranulation. In fact, there was a slight decrease at 15 and 30 minutes, and again at 60 minutes, which was lost at 90 and 120 minutes when compared to control NK92-TCR(DGE) cells (Figure 4.10). A second repeat of the assay was performed to conclude the results.

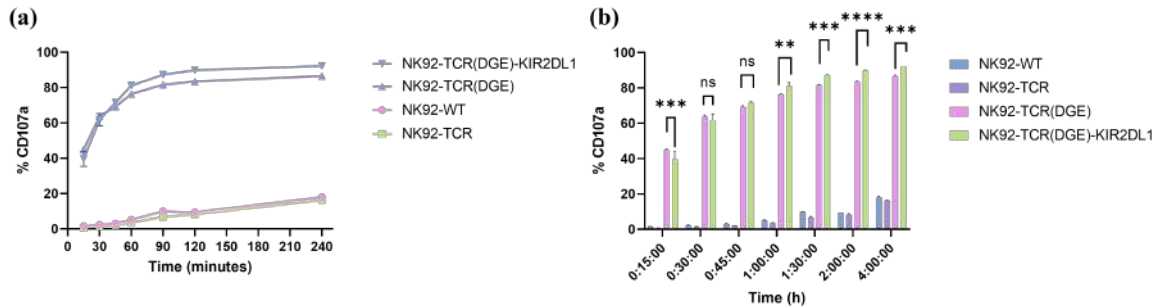


Figure 4.11. Second time-point degranulation assay against A375Tyr cells.

(a) line and (b) bar representation of the time-point degranulation assay. Except for 15-minute time point, KIR2DL1 expressing cells showed higher CD107a levels in comparison to control NK92-TCR(DGE) cells. (Two-way ANOVA analysis. ** $p=0.0019$, *** $p=0.0002$, **** $p<0.0001$).

Repeat of the time point degranulation assay showed that, at later time points, degranulation levels of KIR2DL1 expressing NK92-TCR(DGE) cells reach or surpass the amount of surface CD107a level when compared to NK92-TCR(DGE) cells (Figure 4.11).

4.5.2. Cytotoxic Activity of TCR-NK KIR2DL1 Cells

Measurement of cytotoxic activity of KIR2DL1 expressing cells was measured using a real-time cell analysis (RTCA), based on the electrical impedance of the cells. To assess the detailed dynamics of cytotoxic function of these cells, different effector-to-target ratios were performed.

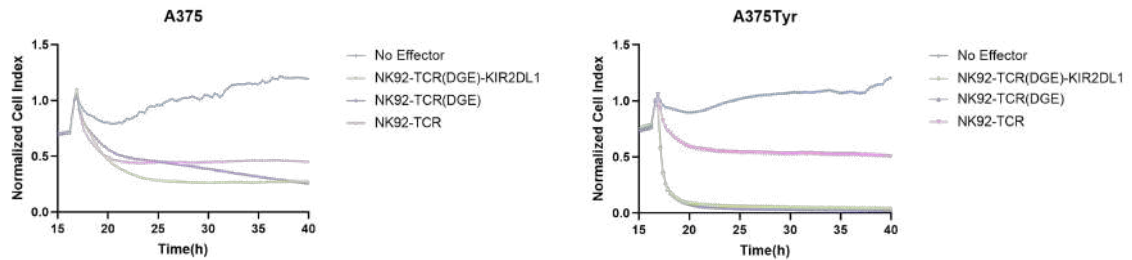


Figure 4.12. Real-time cell analysis of different effector cells against both A375 and A375Tyr cells.

Cell index measurement was carried out for 24 hours following the effector addition at 16 hours. Cell index normalized to 1 at the time of effector cell addition.

As can be seen from Figure 4.12, the normalized cell index of A375Tyr cells is almost the same when they are co-incubated with either NK92-TCR(DGE)-KIR2DL1 or NK92-TCR(DGE) only. Like degranulation, to see whether there is a significant difference at early time points, 1-to-6-hour cell indexes were graphed individually.

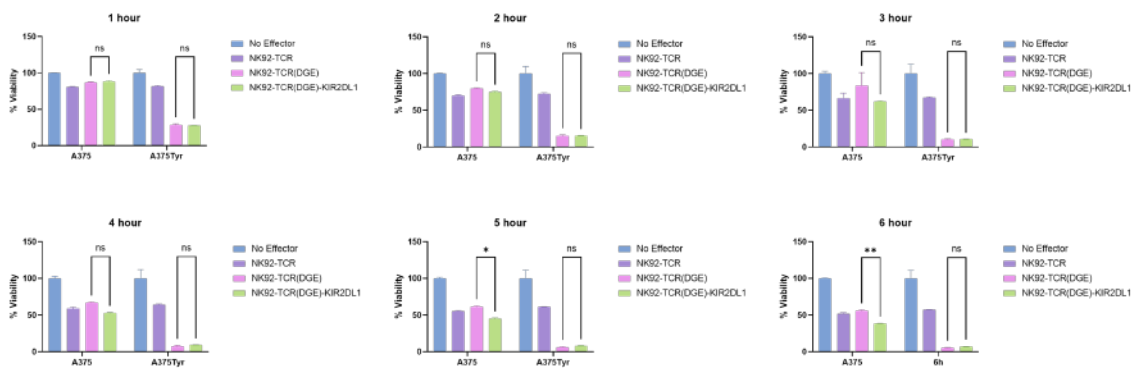


Figure 4.13. 1-to-6-hour timepoints of cell indexes which were baseline-corrected to no effector cell indexes at each hour.

While there were some slight significant differences at different timepoints against A375, further characterization of the cytotoxic function of KIR2DL1 was measured with different effector-to-target ratios. First, 0.1:10 E:T ratio was tried out.

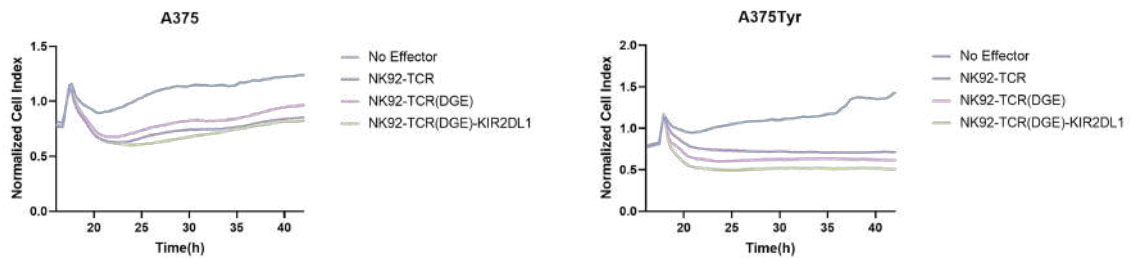


Figure 4.14. RTCA analysis of the effector cells against A375 and A375Tyr at 0.1:10 E:T ratio.

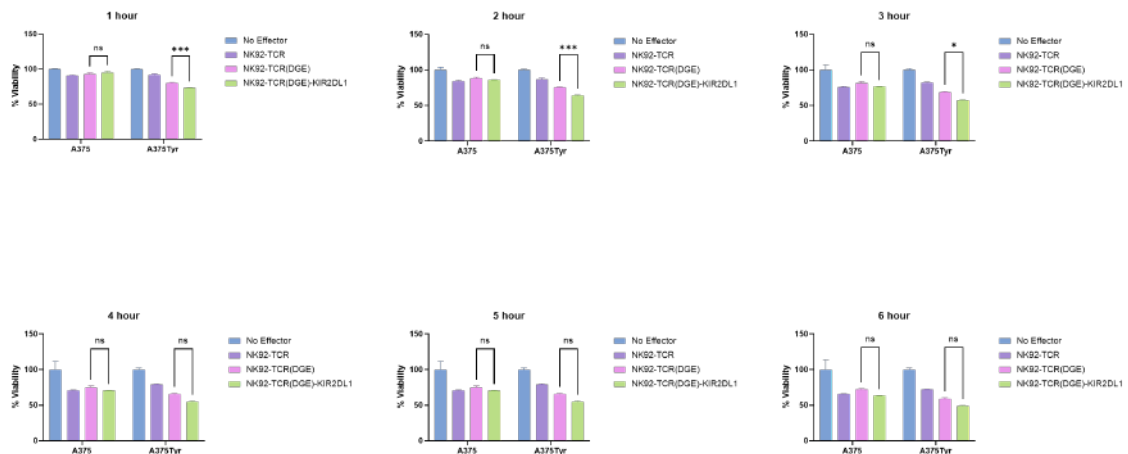


Figure 4.15. 1-to-6-hour timepoints of cell indexes which were baseline-corrected to no effector cell indexes at each hour.

For the first 3 hours, there was a slight increase in terms of cytotoxicity of KIR2DL1 expressing effector cells, however after 4 hours, the difference was no longer significant (Two-way ANOVA analysis. * $p=0.0135$, *** $p=0.0005$ for 2 hour, and $p=0.0009$ for 1 hour, ns=not significant).

Since there was a significant difference observed between NK92-TCR(DGE) and KIR2DL1 expressing NK92-TCR(DGE), another RTCA assay was performed where the effector amount was increased to 0.3:10 E:T ratio.

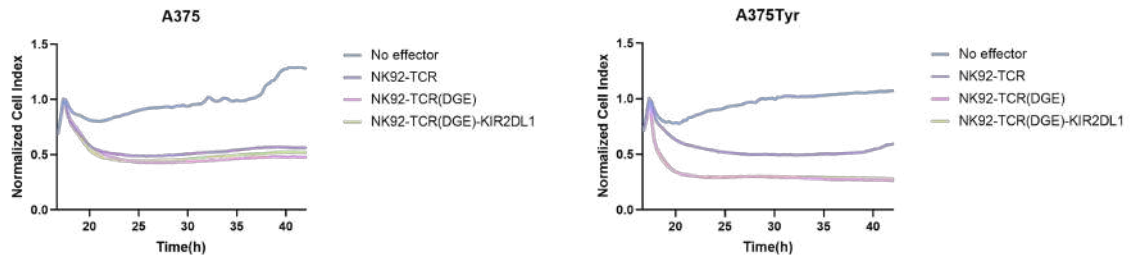


Figure 4.16. RTCA analysis of the effector cells against A375 and A375Tyr at 0.3:10 E:T ratio.

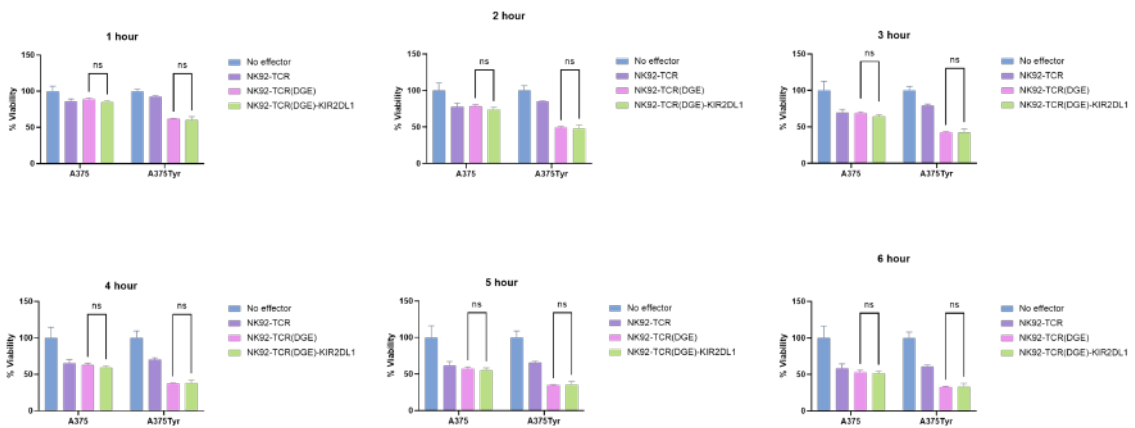


Figure 4.17. 1-to-6-hour timepoints of cell indexes which were baseline-corrected to no effector cell indexes at each hour.

Increased number of KIR2DL1 expressing did not show a significant difference at various timepoints (ns=not significant).

Overall timepoint analysis of 0.3:10 E:T ratio did not show a significant effect mediated through KIR2DL1 expression on the cytotoxicity of TCR expressing NK cells.

While at 1:1 and 0.3:10 ratios KIR2DL1 expressing cells do not show a significant difference, at a very low ratio, 0.1:10, KIR2DL1 expressing NK92-TCR(DGE) cells showed a significant increase in cytotoxic function, and showed a faster response.

4.5.3. TNF- α and IFN- γ Secretion of TCR-NK KIR2DL1 Cells

During NK cell triggering, in addition to degranulation of cytolytic enzymes, NK cells secrete cytokines such as TNF- α and IFN- γ . Here, we have co-incubated effectors with their targets for 4 hours, followed by intracellular staining of either TNF- α or IFN- γ .

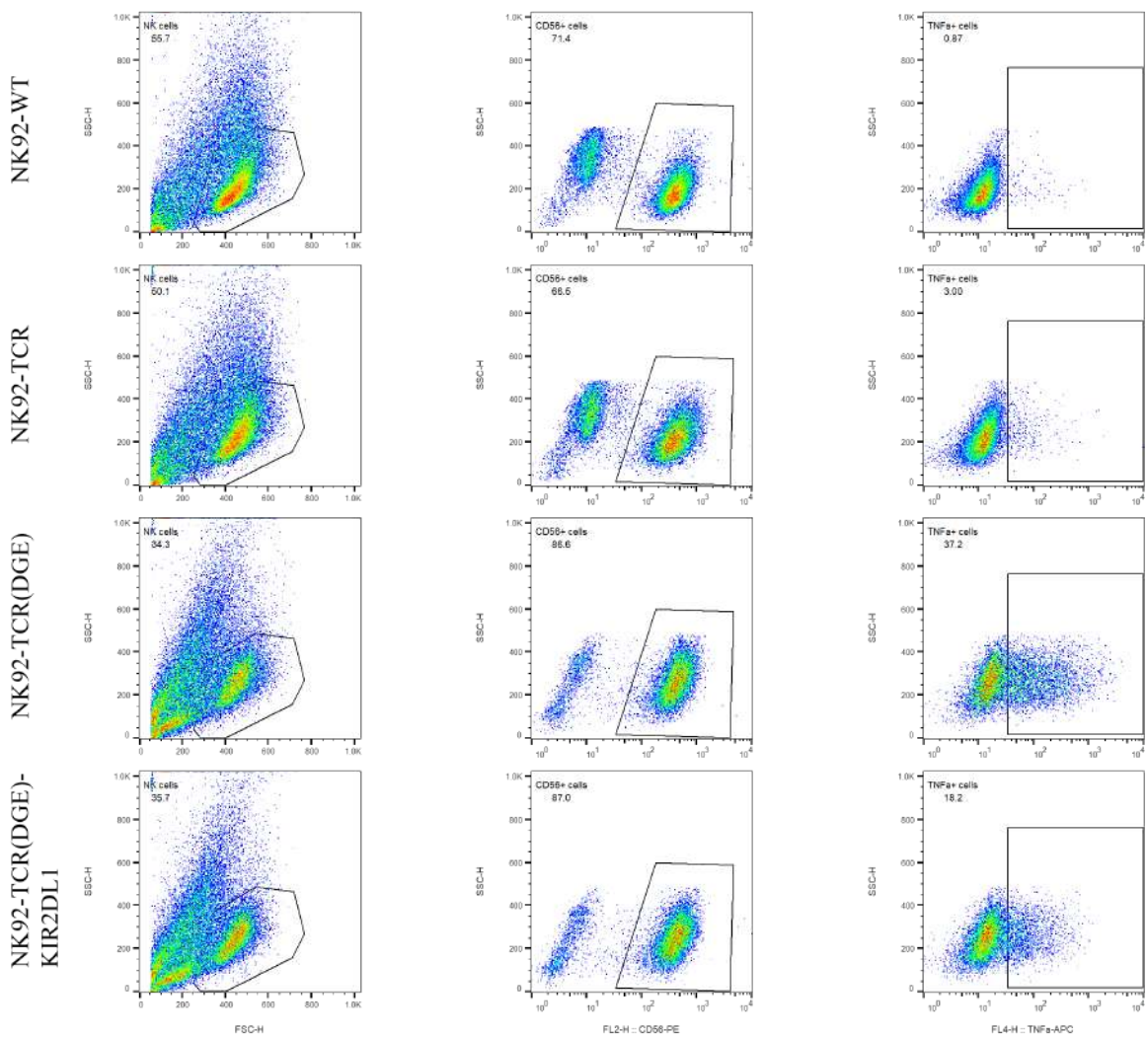


Figure 4.18. TNF- α expression levels in A375Tyr stimulated effector cells.

Here in Figure 4.18, there is an increase of TNF- α expression in both cells that are expressing functional TCRs (NK92-TCR(DGE) and NK92-TCR(DGE)-KIR2DL1) when compared to wild type NK92 or NK92-TCR. However, there is a significant decrease in NK92-TCR(DGE)-KIR2DL1 when compared to NK92-TCR(DGE) (supported in Figure 4.19).

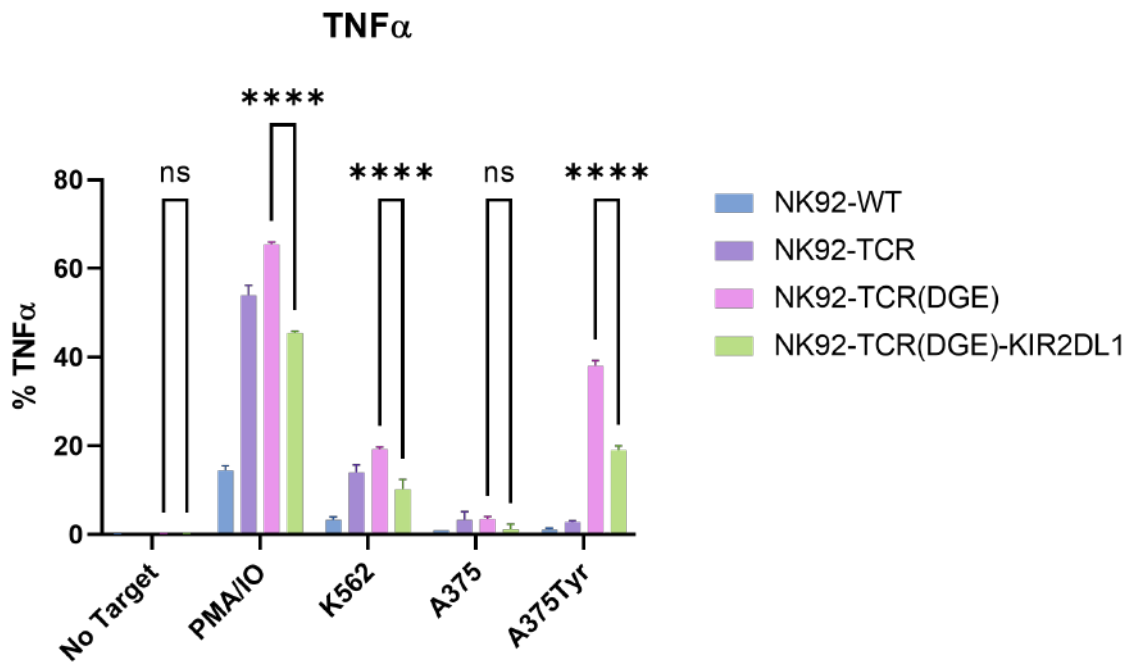


Figure 4.19. Bar graph representation of TNF- α secretion.

In addition to A375Tyr stimulation, KIR2DL1 expressing cells showed significant decrease when they are stimulated chemically (PMA/IO) or with K562 cells. However, A375 cells did not stimulate a significant response in NK92-TCR(DGE)-KIR2DL1 cells (Figure 4.19).

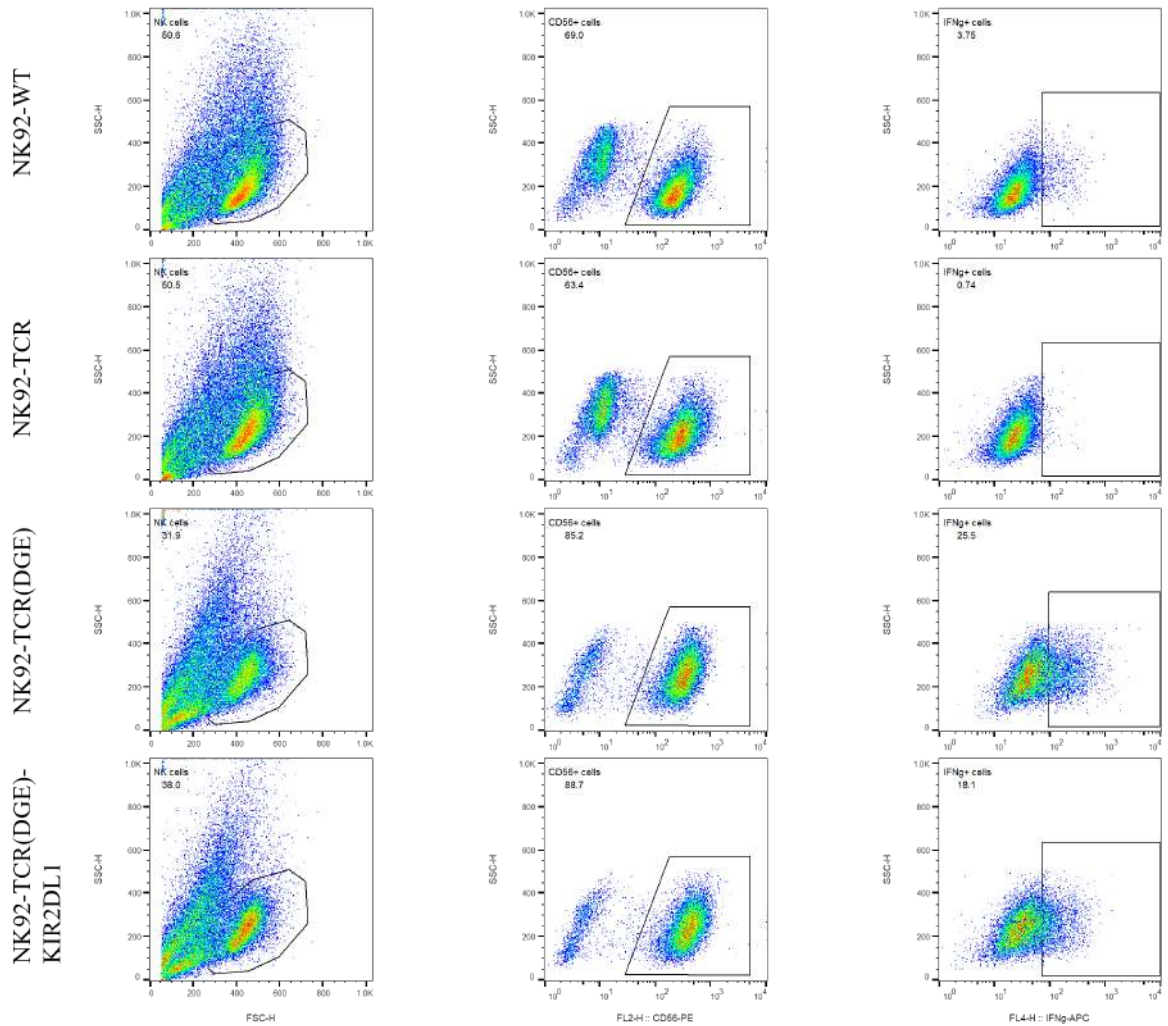


Figure 4.20. IFN- γ expression levels in A375Tyr stimulated effector cells.

In contrast to TNF- α , a decrease in IFN- γ expression between A375Tyr stimulated NK92-TCR(DGE) and NK92-TCR(DGE)-KIR2DL1 cells were not significant. But, similar to TNF- α , functional TCR expression has increased IFN- γ expression compared to wild-type NK92 and NK92-TCR cells against A375Tyr (Figure 4.20).

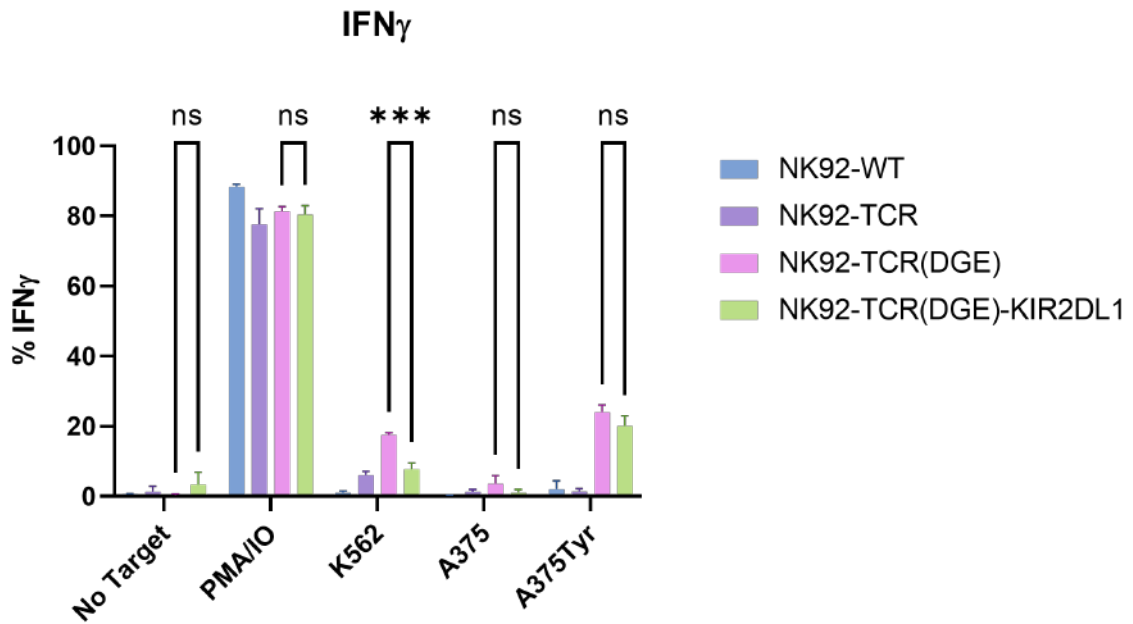


Figure 4.21. Bar graph representation of IFN- γ secretion.

Against all targets, except A375, the decrease observed in KIR2DL1 expressing cells against NK92-TCR(DGE) cells was not significant (Figure 4.21). Overall cytokine secretion assay showed that there might be a KIR2DL1-mediated TNF- α decrease in A375Tyr cells, but the same does not apply to IFN- γ secretion. However, a similar reduction was observed in A375 cells for IFN- γ .

4.5.4. Western Blot Analysis of Phospho-proteins in TCR-NK KIR2DL1 Cells

During NK cell triggering and TCR signaling, various signaling intermediates are phosphorylated, such as PLC γ 1 and Erk1/2. Western blot analysis of these proteins was performed after co-incubation during a given period of time under serum-starved conditions.

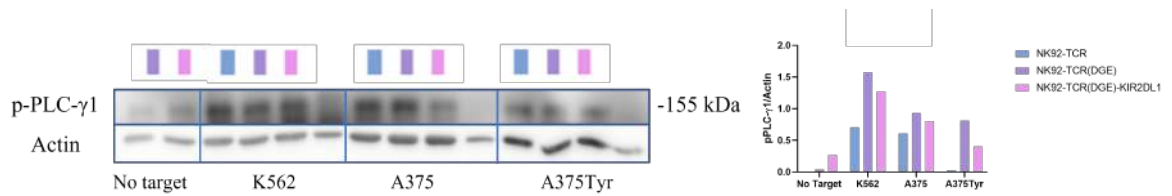


Figure 4.22. Phospho-PLC γ 1 expression levels in stimulated effector cells.

Phospho-PLC γ 1 levels were decreased in KIR2DL1 expressing cells against all targets, as observed in Figure 4.22, both in the image and the quantitative results obtained from normalized values to the respective actin band intensities.

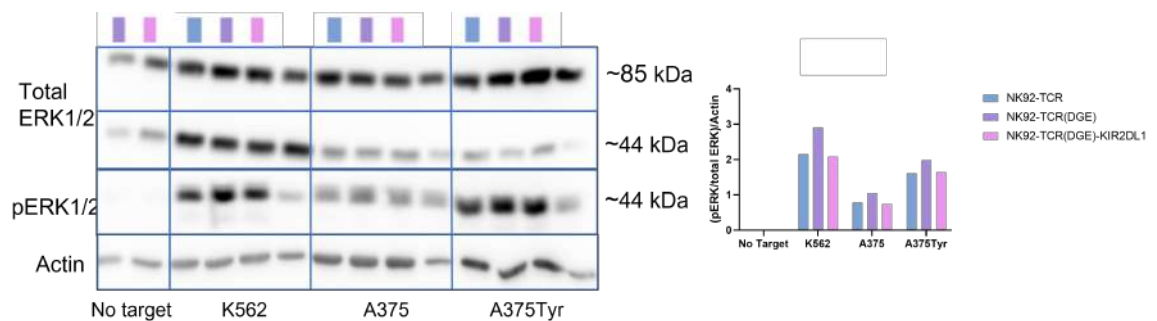


Figure 4.23. PPhospho-Erk1/2 and total Erk expression levels in stimulated effector cells.

Similar to phospho-PLC γ 1 levels, a decrease was observed in the overall phosphorylation of Erk1/2 (Figure 4.23).

5. DISCUSSION

Adoptive immunotherapy relies on our body's own immune cells to fight against cancer. While most adoptive cell therapies are based on T cells through TCR or CAR transfer, many setbacks are present in both cases. For CAR-T cells, the therapy focuses on the tumour antigen expression in the tumour cell, not on the healthy cells. Although it is a successful approach for B cell malignancies through CD19 targeting (Kowolik et al., 2006), loss of the tumour antigen or the lack of identified tumour-specific antigens are still challenges of CAR-T cell therapies. In the case of TCR-T cell therapies, a major setback is the mispairing problem. Genetically modified T cells with TCR $\alpha\beta$ chains can be mispaired with the endogenous β and α TCR chains. Newly mispaired TCR heterodimers can be self-reactive or not elicit a response. However, they can reduce the overall efficacy of targeted TCR therapy (van Loenen et al., 2010).

In the light of these setbacks of T cell-based adoptive cell therapies, NK cells have become a field yet to be explored. Either patient-derived or healthy donor-derived NK cells can be possibly safer for adoptive immunotherapy. However, primary NK cell-based therapies have their own challenges. Patient-derived NK cells are faced with silencing after self-MHC encounters. Due to diverse inhibitory receptor expressions, donor-derived NK cells can initiate acute graft-versus-host disease even though T cells are depleted (Shah et al., 2015). Additionally, primary NK cell retrieval is complex due to low amounts of NK cells in circulation. Following the collection, expansion of these cells in vitro is also a challenge (Alici & Sutlu, 2009).

NK92 is a cell line derived from a Non-Hodgkin's lymphoma patient. It is a highly cytotoxic cell line due to the expression of many activating receptors (NKp46 and 2B4) and the lack of expression of inhibitory receptors (most of the inhibitory KIRs) except the NKG2A-CD94 complex (Gong et al., 1994). The high cytotoxicity of this cell line made them a possible candidate to overcome challenges in T cell-based therapies. With the similar signaling mechanism of NK cells to T cells, their adaptation to the same genetic modifications performed on T cells is inescapable.

While NK cell-based adoptive immunotherapy primarily relied on CAR engineering, their aforementioned shared signaling machinery with T cells made them excellent candidates for TCR engineering. As of now, very few studies have used NK92 cells engineered with TCR (Mensali et al., 2019; Parlar et al., 2019) and showed successful antigen-specific targeting with NK92 cells.

However, molecular dynamics of the TCR with the downstream NK cell activity through inhibitory receptors are unknown. Despite their high cytotoxicity, NK92 cells' requirement of pre-irradiation results in reduced efficacy in therapy. Recently, another group (Morton et al., 2022) has developed TCR expressing primary NK cells that showed NK-cell mediated lysis during HLA class I loss, a concern of TCR-mediated therapies.

While primary NK cell usage is a way to study inhibitory signals and TCR signaling, NK92 cells create a platform where different combinations of each inhibitory KIR can be tested. Hence, in this study, we have used NK92 cells to express the inhibitory KIR receptor KIR2DL1. The ligand for KIR2DL1 is HLA-C2 (Winter et al., 1998), and it is different from our antigen-presenting HLA, HLA-A2, which engineered TCR recognizes. With this, we wanted to create recognition pathways that are distinct from each other and to see whether we can harness these NK cells to have dual targets.

We started this study by first cloning a CD3 subunits vector that does not express any fluorescent protein. Since we already have the NK92 cell line expressing a TCR recognizing the tyrosinase epitope expressed by A375 melanoma cells, we transduced these NK92-TCR cells with CD3 subunits, for no surface TCR expression can be obtained in the absence of CD3 subunits. All the transductions were carried out in the presence of a TAK1 inhibitor, (5Z)-7-Oxozeaenol, to increase the NK92 cell transduction by inhibiting the intracellular antiviral defense mechanism.

After obtaining the final effector TCR-NK cells expressing KIR2DL1, the degranulation capacity of these cells was measured against targets. Cells were either stimulated chemically by PMA/IO or with their natural cell target, K562, a cell line lacking HLA expression. While the KIR2DL1 expressing cells are successfully triggered by these control groups, overall CD107a levels have shown significant increases in all targets, indicating an increase in cytotoxicity without the antigen-specific response.

Similar high cytotoxicity was observed within the RTCA assays, although not significant. Since additional expression of an inhibitory receptor was expected to result in decrease in degranulation and cytotoxicity, the effect of KIR2DL1 on TCR-NK signaling is still a question.

To follow up on the degranulation and cytotoxicity, molecular downstream effects of the KIR2DL1 were investigated with a phospho-protein analysis. PLC γ 1 and Erk1/2 are phosphorylated during TCR activation and downstream of KIR signaling (Gaud et al., 2018). The Western blot results showed a different story when compared to degranulation and cytotoxicity assays, where we observed decreases in both phospho-protein levels. However, a decreasing trend was observed in all targets, including the K562 cells that do not express the melanoma antigen.

Similar to immunoblotting, a decrease in the cytokine secretion profile of TCR-NK cells expressing KIRs was observed. It has been stated previously that cytokine secretion of NK cells is linked with their cytolytic activity (Wang et al., 2012). However, both IFN- γ and TNF- α levels have reduced KIR2DL1 expressing cells. It has been reported that TNF- α can contribute to IFN- γ production in NK cells (Almishri et al., 2016), so the overall cytokine secretion profile may be comparable. However, the negative correlation between cytotoxicity, cytokine secretion, and signaling inclines us to postulate other outcomes.

Overexpression of many genes on NK cells can alter their phenotypes, resulting in an overexpression of activating signals. Since these receptors balance the NK cell cytotoxicity, the overall sum of activating receptors can overcome the overexpressed

single inhibitory receptor. Although there seem to be further explanations required, TCR-NK cells that express inhibitory KIR receptors can work synergistically with TCR signaling. However, as further studies, granzyme B and perforin loads of these KIR2DL1 expressing TCR-NK cells must be investigated to see whether these TCR-NK cells that previously lacked inhibitory expression could undergo a process similar to NK cell education. Additionally, phospho-protein levels of other signaling intermediates such as Vav1, LAT, SLP-76, and PKC θ which are extremely important in both TCR and KIR signaling can be measured.

6. REFERENCES

Adams, N. M., S. Grassmann and J. C. Sun, “Clonal Expansion of Innate and Adaptive Lymphocytes”, *Nature Reviews Immunology*, Vol. 20, No. 11, pp. 694–707, 2020.

Alici, E., and T. Sutlu, “Natural Killer Cell-Based Immunotherapy in Cancer: Current Insights and Future Prospects”, *Journal of Internal Medicine*, Vol. 266, No. 2, pp. 154–181, 2009.

Almishri, W., T. Santodomingo-Garzon, T. Le, D. Stack, C. H. Mody and M. G. Swain, “TNF α Augments Cytokine-Induced NK Cell IFN γ Production through TNFR2”, *Journal of Innate Immunity*, Vol. 8, No. 6, pp. 617–629, 2016.

Anderson, M. E., and T. J. Siahaan, “Targeting ICAM-1/LFA-1 Interaction for Controlling Autoimmune Diseases: Designing Peptide and Small Molecule Inhibitors”, *Peptides*, Vol. 24, No. 3, pp. 487–501, 2003.

Anfossi, N., P. André, S. Guia, C. S. Falk, S. Roetynck, C. A. Stewart, V. Bresó, C. Frassati, D. Reviron, D. Middleton, F. Romagné, S. Ugolini and E. Vivier, “Human NK Cell Education by Inhibitory Receptors for MHC Class I”, *Immunity*, Vol. 25, No. 2, pp. 331–342, 2006.

Bhatt, R. S., A. Berjis, J. C. Konge, K. M. Mahoney, A. N. Klee, S. S. Freeman, C. H. Chen, O. A. Jegede, P. J. Catalano, J. C. Pignon, M. Sticco-Ivins, B. Zhu, P. Hua, J. Soden, J. Zhu, D. F. McDermott, A. R. Arulanandam, S. Signoretti and G. J. Freeman, “KIR3DL3 Is an Inhibitory Receptor for HHLA2 That Mediates an Alternative Immunoinhibitory Pathway to PD1”, *Cancer Immunology Research*, Vol. 9, No. 2, pp. 156, 2021.

Boehm, U., T. Klamp, M. Groot and J. C. Howard, “Cellular Responses to Interferon-Gamma”, *Annual Review of Immunology*, Vol. 15, , pp. 749–795, 1997.

Braud, V. M., D. S. J. Allan, C. A. O’Callaghan, K. Soderstrom, A. D’Andrea, G. S. Ogg, S. Lazetic, N. T. Young, J. I. Bell, J. H. Phillips, L. L. Lanler and A. J. McMichael, “HLA-E Binds to Natural Killer Cell Receptors CD94/NKG2A, B and C”, *Nature*, Vol. 391, No. 6669, pp. 795–799, 1998.

Burnet, F. M., “A Modification of Jerne’s Theory of Antibody Production Using the Concept of Clonal Selection.”, *Australian Journal of Science*, Vol. 20, No. 3, pp. 67–69, 1957.

Cantrell, D. A., “T-Cell Antigen Receptor Signal Transduction”, *Immunology*, Vol. 105, No. 4, pp. 369, 2002.

Cooper, M. A., T. A. Fehniger and M. A. Caligiuri, “The Biology of Human Natural Killer-Cell Subsets”, *Trends in Immunology*, Vol. 22, No. 11, pp. 633–640, 2001.

Cooper, M. D., and M. N. Alder, “The Evolution of Adaptive Immune Systems”, *Cell*, Vol. 124, No. 4, pp. 815–822, 2006.

Eshhar, Z., and G. Gross, “Chimeric T Cell Receptor Which Incorporates the Anti-Tumour Specificity of a Monoclonal Antibody with the Cytolytic Activity of T Cells: A Model System for Immunotherapeutical Approach.”, *The British Journal of Cancer. Supplement*, Vol. 10, No. SUPPL. X, pp. 27, 1990.

Fallon, P. G., H. E. Jolin, P. Smith, C. L. Emson, M. J. Townsend, R. Fallon, P. Smith and A. N. J. McKenzie, “IL-4 Induces Characteristic Th2 Responses Even in the Combined Absence of IL-5, IL-9, and IL-13”, *Immunity*, Vol. 17, No. 1, pp. 7–17, 2002.

Feske, S., “Calcium Signalling in Lymphocyte Activation and Disease”, *Nature Reviews Immunology*, Vol. 7, No. 9, pp. 690–702, 2007.

Fittje, P., A. Hoelzemer, W. F. Garcia-Beltran, S. Vollmers, A. Niehrs, K. Hagemann, G. Martrus, C. Kö Rner, F. Kirchhoff, D. Sauter and M. Altfeldid, “HIV-1 Nef-Mediated Downregulation of CD155 Results in Viral Restriction by KIR2DL5+ NK Cells”, *PLOS Pathogens*, Vol. 18, No. 6, pp. e1010572, 2022.

Gaud, G., R. Lesourne and P. E. Love, “Regulatory Mechanisms in T Cell Receptor Signalling”, *Nature Reviews Immunology*, Vol. 18, No. 8, pp. 485–497, 2018.

Genot, E., and D. A. Cantrell, “Ras Regulation and Function in Lymphocytes”, *Current Opinion in Immunology*, Vol. 12, No. 3, pp. 289–294, 2000.

Germain, R. N., “T-Cell Development and the CD4–CD8 Lineage Decision”, *Nature Reviews Immunology*, Vol. 2, No. 5, pp. 309–322, 2002.

Germain, R. N., and D. H. Margulies, “The Biochemistry and Cell Biology and Antigen Processing and Presentation”, *Annual Review of Immunology*, Vol. 11, , pp. 403–450, 1993.

Gong, J. H., G. Maki and H. G. Klingemann, “Characterization of a Human Cell Line (NK-92) with Phenotypical and Functional Characteristics of Activated Natural Killer Cells.”, *Leukemia*, Vol. 8, No. 4, pp. 652–658, 1994.

Gross, O., C. Grupp, C. Steinberg, S. Zimmermann, D. Strasser, N. Hanneschläger, W. Reindl, H. Jonsson, H. Huo, D. R. Littman, C. Peschel, W. M. Yokoyama, A. Krug and J. Ruland, “Multiple ITAM-Coupled NK-Cell Receptors Engage the Bcl10/Malt1 Complex via Carma1 for NF-KB and MAPK Activation to Selectively Control Cytokine Production”, *Blood*, Vol. 112, No. 6, pp. 2421, 2008.

Gumperz, J. E., V. Litwin, J. H. Phillips, L. L. Lanier and P. Parham, “The Bw4 Public Epitope of HLA-B Molecules Confers Reactivity with Natural Killer Cell Clones That Express NKB1, a Putative HLA Receptor”, *The Journal of Experimental Medicine*, Vol. 181, No. 3, pp. 1133, 1995.

Hanna, J., P. Bechtel, Y. Zhai, F. Youssef, K. McLachlan and O. Mandelboim, “Novel Insights on Human NK Cells’ Immunological Modalities Revealed by Gene Expression Profiling”, *The Journal of Immunology*, Vol. 173, No. 11, pp. 6547–6563, 2004.

Hewitt, E. W., “The MHC Class I Antigen Presentation Pathway: Strategies for Viral Immune Evasion”, *Immunology*, Vol. 110, No. 2, pp. 163, 2003.

Hsu, K. C., S. Chida, D. E. Geraghty and B. Dupont, “The Killer Cell Immunoglobulin-like Receptor (KIR) Genomic Region: Gene-Order, Haplotypes and Allelic Polymorphism”, *Immunological Reviews*, Vol. 190, No. 1, pp. 40–52, 2002.

Janeway, C. A., “Approaching the Asymptote? Evolution and Revolution in Immunology”, *Cold Spring Harbor Symposia on Quantitative Biology*, Vol. 54 Pt 1, No. 1, pp. 1–13, 1989.

Janeway, C. A., and R. Medzhitov, “Innate Immune Recognition”, *Annual Review of Immunology*, Vol. 20, , pp. 197–216, 2002.

Jiang, K., B. Zhong, D. L. Gilvary, B. C. Corliss, E. Hong-Geller, S. Wei and J. Y. Djeu, “Pivotal Role of Phosphoinositide-3 Kinase in Regulation of Cytotoxicity in Natural Killer Cells”, *Nature Immunology*, Vol. 1, No. 5, pp. 419–425, 2000.

Kärre, K., H. G. Ljunggren, G. Piontek and R. Kiessling, “Selective Rejection of H-2-Deficient Lymphoma Variants Suggests Alternative Immune Defence Strategy”, *Nature*, Vol. 319, No. 6055, pp. 675–678, 1986.

Kloetzel, P. M., “Generation of Major Histocompatibility Complex Class I Antigens: Functional Interplay between Proteasomes and TPP1”, *Nature Immunology*, Vol. 5, No. 7, pp. 661–669, 2004.

Kowolik, C. M., M. S. Topp, S. Gonzalez, T. Pfeiffer, S. Olivares, N. Gonzalez, D. D. Smith, S. J. Forman, M. C. Jensen and L. J. N. Cooper, “CD28 Costimulation Provided through a CD19-Specific Chimeric Antigen Receptor Enhances in Vivo Persistence and Antitumor Efficacy of Adoptively Transferred T Cells”, *Cancer Research*, Vol. 66, No. 22, pp. 10995–11004, 2006.

Kuball, J., M. L. Dossett, M. Wolf, W. Y. Ho, R. H. Voss, C. Fowler and P. D. Greenberg, “Facilitating Matched Pairing and Expression of TCR Chains Introduced into Human T Cells”, *Blood*, Vol. 109, No. 6, pp. 2331, 2007.

Kumar, S., “Natural Killer Cell Cytotoxicity and Its Regulation by Inhibitory Receptors”, *Immunology*, Vol. 154, No. 3, pp. 383–393, 2018.

Kumar, B. v., T. J. Connors and D. L. Farber, “Human T Cell Development, Localization, and Function throughout Life”, *Immunity*, Vol. 48, No. 2, pp. 202, 2018.

Land, W., “Allograft Injury Mediated by Reactive Oxygen Species: From Conserved Proteins of Drosophila to Acute and Chronic Rejection of Human Transplants. Part III: Interaction of (Oxidative) Stress-Induced Heat Shock Proteins with Toll-like Receptor-Bearing Cells”, *Transplantation Reviews*, Vol. 17, No. 2, pp. 67–86, 2003.

Lanier, L. L., “On Guard - Activating NK Cell Receptors”, *Nature Immunology*, Vol. 2, No. 1, pp. 23–27, 2001.

Lanier, L. L., “Natural Killer Cell Receptor Signaling”, *Current Opinion in Immunology*, Vol. 15, No. 3, pp. 308–314, 2003.

Lanier, L. L., “NK Cell Recognition”, *Annual Review of Immunology*, Vol. 23, , pp. 225–274, 2005.

Lanier, L. L., “Up on the Tightrope: Natural Killer Cell Activation and Inhibition”, *Nature Immunology*, Vol. 9, No. 5, pp. 495–502, 2008.

Lanier, L. L., B. C. Cortiss, J. Wu, C. Leong and J. H. Phillips, “Immunoreceptor DAP12 Bearing a Tyrosine-Based Activation Motif Is Involved in Activating NK Cells”, *Nature*, Vol. 391, No. 6668, pp. 703–707, 1998. Lewis, R. S., “Calcium Signaling Mechanisms in T Lymphocytes”, *Annual Review of Immunology*, Vol. 19, , pp. 497–521, 2001.

Ljunggren, H. G., and K. Kärre, “In Search of the ‘Missing Self’: MHC Molecules and NK Cell Recognition”, *Immunology Today*, Vol. 11, No. C, pp. 237–244, 1990.

Long, E. O., “Regulation of Immune Responses through Inhibitory Receptors”, *Annual Review of Immunology*, Vol. 17, , pp. 875–904, 1999.

Long, E. O., M. Colonna and L. L. Lanier, “Inhibitory MHC Class I Receptors on NK and T Cells: A Standard Nomenclature”, *Immunology Today*, Vol. 17, No. 2, pp. 100, 1996.

Maki, G., H. G. Klingemann, J. A. Martinson and Y. K. Tam, “Factors Regulating the Cytotoxic Activity of the Human Natural Killer Cell Line, NK-92”, *Journal of Hematotherapy and Stem Cell Research*, Vol. 10, No. 3, pp. 369–383, 2001.

Martin, A. M., E. M. Freitas, C. S. Witt, F. T. Christiansen, A. M. Martin, E. M. Freitas, C. S. Witt and F. T. Christiansen, “The Genomic Organization and Evolution of the Natural Killer Immunoglobulin-like Receptor (KIR) Gene Cluster”, *Immunogenetics*, Vol. 51, , pp. 268–280, 2000.

Matzinger, P., “Tolerance, Danger, and the Extended Family”, *Annual Review of Immunology*, Vol. 12, , pp. 991–1045, 1994.

Medjouel Khelifi, H., S. Guia, E. Vivier and E. Narni-Mancinelli, “Role of the ITAM-Bearing Receptors Expressed by Natural Killer Cells in Cancer”, *Frontiers in Immunology*, Vol. 0, , pp. 2256, 2022.

Medzhitov, R., “Recognition of Microorganisms and Activation of the Immune Response”, *Nature*, Vol. 449, No. 7164, pp. 819–826, 2007.

Medzhitov, R., and C. Jr. Janeway, “Innate Immunity”, *The New England Journal of Medicine*, Vol. 343, No. 5, pp. 338–344, 2009.

Mensali, N., P. Dillard, M. Hebeisen, S. Lorenz, T. Theodossiou, M. R. Myhre, A. Fåne, G. Gaudernack, G. Kvalheim, J. H. Myklebust, E. M. Inderberg and S. Wälchli, “NK Cells Specifically TCR-Dressed to Kill Cancer Cells”, *EBioMedicine*, Vol. 40, , pp. 106, 2019.

Moretta, L., R. Biassoni, C. Bottino, C. Cantoni, D. Pende, M. C. Mingari and A. Moretta, “Human NK Cells and Their Receptors”, *Microbes and Infection*, Vol. 4, No. 15, pp. 1539–1544, 2002.

Morgan, R. A., M. E. Dudley, J. R. Wunderlich, M. S. Hughes, J. C. Yang, R. M. Sherry, R. E. Royal, S. L. Topalian, U. S. Kammula, N. P. Restifo, Z. Zheng, A. Nahvi, C. R. de Vries, L. J. Rogers-Freezer, S. A. Mavroukakis and S. A. Rosenberg, “Cancer Regression in Patients after Transfer of Genetically Engineered Lymphocytes”, *Science*, Vol. 314, No. 5796, pp. 126–129, 2006.

Morton, L. T., T. L. A. Wachsmann, M. H. Meeuwssen, A. K. Wouters, D. F. G. Remst, M. M. van Loenen, J. H. F. Falkenburg and M. H. M. Heemskerk, “T Cell Receptor Engineering of Primary NK Cells to Therapeutically Target Tumors and Tumor Immune Evasion”, *Journal for ImmunoTherapy of Cancer*, Vol. 10, No. 3, pp. e003715, 2022.

Mosmann, T. R., H. Cherwinski, M. W. Bond, M. A. Giedlin and R. L. Coffman, “Two Types of Murine Helper T Cell Clone. I. Definition According to Profiles of Lymphokine Activities and Secreted Proteins.”, *Journal of Immunology*, Vol. 136, No. 7, pp. 2348–2357, 1986.

Palucka, K., and J. Banchereau, “Linking Innate and Adaptive Immunity”, *Nature Medicine*, Vol. 5, No. 8, pp. 868–870, 1999.

Park, H., Z. Li, X. O. Yang, S. H. Chang, R. Nurieva, Y. H. Wang, Y. Wang, L. Hood, Z. Zhu, Q. Tian and C. Dong, “A Distinct Lineage of CD4 T Cells Regulates Tissue Inflammation by Producing Interleukin 17”, *Nature Immunology*, Vol. 6, No. 11, pp. 1133–1141, 2005.

Parkin, J., and B. Cohen, “An Overview of the Immune System”, *The Lancet*, Vol. 357, No. 9270, pp. 1777–1789, 2001.

Parlar, A., E. C. Sayitoglu, D. Ozkazanc, A. M. Georgoudaki, C. Pamukcu, M. Aras, B. J. Josey, M. Chrobok, S. Branecki, P. Zahedimaram, L. Ikromzoda, E. Alici, B. Erman, A. D. Duru and T. Sutlu, “Engineering Antigen-Specific NK Cell Lines against the Melanoma-Associated Antigen Tyrosinase via TCR Gene Transfer”, *European Journal of Immunology*, Vol. 49, No. 8, pp. 1278–1290, 2019.

Pende, D., R. Biassoni, C. Cantoni, S. Verdiani, M. Falco, C. di Donato, L. Accame, C. Bottino, A. Moretta and L. Moretta, “The Natural Killer Cell Receptor Specific for HLA-A Allotypes: A Novel Member of the P58/P70 Family of Inhibitory Receptors That Is Characterized by Three Immunoglobulin-like Domains and Is Ex-

pressed as a 140-KD Disulphide-Linked Dimer”, *Journal of Experimental Medicine*, Vol. 184, No. 2, pp. 505–518, 1996.

Pende, D., M. Falco, M. Vitale, C. Cantoni, C. Vitale, E. Munari, A. Bertaina, F. Moretta, G. del Zotto, G. Pietra, M. C. Mingari, F. Locatelli and L. Moretta, “Killer Ig-like Receptors (KIRs): Their Role in NK Cell Modulation and Developments Leading to Their Clinical Exploitation”, *Frontiers in Immunology*, Vol. 10, No. MAY, pp. 1179, 2019.

Rajagopalan, S., and E. O. Long, “A Human Histocompatibility Leukocyte Antigen (HLA)-G-Specific Receptor Expressed on All Natural Killer Cells”, *Journal of Experimental Medicine*, Vol. 189, No. 7, pp. 1093–1100, 1999.

Raphael, I., S. Nalawade, T. N. Eagar and T. G. Forsthuber, “T Cell Subsets and Their Signature Cytokines in Autoimmune and Inflammatory Diseases”, *Cytokine*, Vol. 74, No. 1, pp. 5, 2015.

Ravetch, J. v., and L. L. Lanier, “Immune Inhibitory Receptors”, *Science*, Vol. 290, No. 5489, pp. 84–89, 2000.

Reinherz, E. L., “A β TCR-Mediated Recognition: Relevance to Tumor-Antigen and Cancer Immunotherapy”, *Cancer Immunology Research*, Vol. 3, No. 4, pp. 305, 2015.

Reinherz, E. L., S. C. Meuer and S. F. Schlossman, “The Delineation of Antigen Receptors on Human T Lymphocytes”, *Immunology Today*, Vol. 4, No. 1, pp. 5–8, 1983.

Ruggeri, L., M. Capanni, E. Urbani, K. Perruccio, W. D. Shlomchik, A. Tosti, S. Posati, D. Rogaia, F. Frassoni, F. Aversa, M. F. Martelli and A. Velardi, “Effectiveness of Donor Natural Killer Cell Alloreactivity in Mismatched Hematopoietic Transplants”, *Science*, Vol. 295, No. 5562, pp. 2097–2100, 2002.

Schatz, D. G., and Y. Ji, “Recombination Centres and the Orchestration of V(D)J Recombination”, *Nature Reviews Immunology*, Vol. 11, No. 4, pp. 251–263, 2011.

Sebestyén, Z., E. Schooten, T. Sals, I. Zaldivar, E. San José, B. Alarcón, S. Bobisse, A. Rosato, J. Szöllösi, J. W. Gratama, R. A. Willemsen and R. Debets, “Human TCR That Incorporate CD3zeta Induce Highly Preferred Pairing between TCRalpha and Beta Chains Following Gene Transfer”, *Journal of Immunology*, Vol. 180, No. 11, pp. 7736–7746, 2008.

Shah, N. N., K. Baird, C. P. Delbrook, T. A. Fleisher, M. E. Kohler, S. Rampaap, K. Lemberg, C. K. Hurley, D. E. Kleiner, M. S. Merchant, S. Pittaluga, M. Sabatino, D. F. Stroncek, A. S. Wayne, H. Zhang, T. J. Fry and C. L. Mackall, “Acute GVHD in Patients Receiving IL-15/4-1BBL Activated NK Cells Following T-Cell-Depleted Stem Cell Transplantation”, *Blood*, Vol. 125, No. 5, pp. 784–792, 2015.

Shao, H., W. Zhang, Q. Hu, F. Wu, H. Shen and S. Huang, “TCR Mispairing in Genetically Modified T Cells Was Detected by Fluorescence Resonance Energy Transfer”, *Molecular Biology Reports*, Vol. 37, No. 8, pp. 3951–3956, 2010.

Shimasaki, N., H. Fujisaki, D. Cho, M. Masselli, T. Lockey, P. Eldridge, W. Leung and D. Campana, “A Clinically Adaptable Method to Enhance the Cytotoxicity of Natural Killer Cells against B-Cell Malignancies”, *Cytotherapy*, Vol. 14, No. 7, pp. 830–840, 2012.

Sommermeier, D., J. Neudorfer, M. Weinhold, M. Leisegang, B. Engels, E. Noessner, M. H. M. Heemskerk, J. Charo, D. J. Schendal, T. Blankenstein, H. Bernhard and W. Uckert, “Designer T Cells by T Cell Receptor Replacement”, *European Journal of Immunology*, Vol. 36, No. 11, pp. 3052–3059, 2006.

Sprent, J., and D. F. Tough, “Lymphocyte Life-Span and Memory”, *Science*, Vol. 265, No. 5177, pp. 1395–1400, 1994.

Stebbins, C. C., C. Watzl, D. D. Billadeau, P. J. Leibson, D. N. Burshtyn and E. O. Long, “Vav1 Dephosphorylation by the Tyrosine Phosphatase SHP-1 as a Mechanism for Inhibition of Cellular Cytotoxicity”, *Molecular and Cellular Biology*, Vol. 23, No. 17, pp. 6291–6299, 2003.

Steinman, R. M., and M. D. Witmer, “Lymphoid Dendritic Cells Are Potent Stimulators of the Primary Mixed Leukocyte Reaction in Mice”, *Proceedings of the National Academy of Sciences of the United States of America*, Vol. 75, No. 10, pp. 5132–5136, 1978.

Stern, L. J., and D. C. Wiley, “Antigenic Peptide Binding by Class I and Class II Histocompatibility Proteins”, *Structure*, Vol. 2, No. 4, pp. 245–251, 1994.

Topham, N. J., and E. W. Hewitt, “Natural Killer Cell Cytotoxicity: How Do They Pull the Trigger?”, *Immunology*, Vol. 128, No. 1, pp. 7, 2009.

Trapani, J. A., “Target Cell Apoptosis Induced by Cytotoxic T Cells and Natural Killer Cells Involves Synergy between the Pore-Forming Protein, Perforin, and the Serine Protease, Granzyme B”, *Australian and New Zealand Journal of Medicine*, Vol. 25, No. 6, pp. 793–799, 1995.

Trinchieri, G., “Biology of Natural Killer Cells”, *Advances in Immunology*, Vol. 47, No. C, pp. 187–376, 1989.

van Loenen, M. M., R. de Boer, A. L. Amir, R. S. Hagedoorn, G. L. Volbeda, R. Willemze, J. J. van Rood, J. H. F. Falkenburg and M. H. M. Heemskerk, “Mixed T Cell Receptor Dimers Harbor Potentially Harmful Neoreactivity”, *Proceedings of the National Academy of Sciences of the United States of America*, Vol. 107, No. 24, pp. 10972–10977, 2010.

Vivier, E., J. A. Nunès and F. Vély, “Natural Killer Cell Signaling Pathways”, *Science*, Vol. 306, No. 5701, pp. 1517–1519, 2004a.

Vivier, E., J. A. Nunès and F. Vély, “Natural Killer Cell Signaling Pathways”, *Science*, Vol. 306, No. 5701, pp. 1517–1519, 2004b.

Vivier, E., E. Tomasello, M. Baratin, T. Walzer and S. Ugolini, “Functions of Natural Killer Cells”, *Nature Immunology*, Vol. 9, No. 5, pp. 503–510, 2008.

Wang, R., J. J. Jaw, N. C. Stutzman, Z. Zou and P. D. Sun, “Natural Killer Cell-Produced IFN- γ and TNF- α Induce Target Cell Cytolysis through up-Regulation of ICAM-1”, *Journal of Leukocyte Biology*, Vol. 91, No. 2, pp. 299, 2012.

Watts, C., “The Exogenous Pathway for Antigen Presentation on Major Histocompatibility Complex Class II and CD1 Molecules”, *Nature Immunology*, Vol. 5, No. 7, pp. 685–692, 2004.

Wieczorek, M., E. T. Abualrous, J. Sticht, M. Álvaro-Benito, S. Stolzenberg, F. Noé and C. Freund, “Major Histocompatibility Complex (MHC) Class I and MHC Class II Proteins: Conformational Plasticity in Antigen Presentation”, *Frontiers in Immunology*, Vol. 8, No. MAR, pp. 292, 2017.

Winter, C. C., J. E. Gumperz, P. Parham, E. O. Long and N. Wagtmann, “Direct Binding and Functional Transfer of NK Cell Inhibitory Receptors Reveal Novel Patterns of HLA-C Allotype Recognition”, *The Journal of Immunology*, Vol. 161, No. 2, 1998.

APPENDIX A: CHEMICALS

Table A.1: Chemicals used in this study

Chemicals	Company
Acrylamide/Bis-acrylamide, 30% solution	Sigma, Germany
Agar	Sigma, Germany
Agarose	Sigma, Germany
Ammonium per sulphate	Sigma, Germany
Ampicillin	Sigma, Germany
Boric Acid	Sigma, Germany
Bovine Serum Albumin (BSA)	Sigma, Germany
Brefeldin-A	Biolegend, USA
Chloroquine	Sigma, Germany
Distilled Water	Merck Milipore, USA
DMEM	GIBCO, USA Cytiva, UK
DMSO	Sigma, Germany
DNA Gel Loading Dye, 6X	New England Biolabs, USA
DPBS	Cytiva, UK
EDTA	Sigma, Germany
Ethanol	Sigma, Germany
Ethidium Bromide	Sigma, Germany
HEPES solution, 1M	Sigma, Germany
Interleukin-2	Novartis, USA
Ionomycin	Sigma, Germany
Isopropanol	Sigma, Germany
LB Broth	Sigma, Germany
L-Glutamine 200 mM	Cytiva,UK

Table A.1: Chemicals used in this study (cont.)

MEM Vitamin Solution 100X	GIBCO, USA
MEM Non-essential Amino Acid solution 100X	GIBCO, USA
2-Mercaptoethanol	Sigma, Germany
Methanol	Sigma, Germany
Monensin	Biolegend, USA
NaCl	Sigma, Germany
(5Z)-7-Oxozeaenol	Sigma, Germany
Penicillin-Streptomycin	Sigma, Germany
Paraformaldehyde	Biolegend, USA
Phorbol 12-myristate 13-acetate (PMA)	Sigma, Germany
PIPES	Sigma, Germany
Protamine Sulphate	GIBCO, USA
RPMI-1640	Cytiva, UK
Sodium dodecyl sulphate	Sigma, Germany
N,N,N',N'Tetramethylethylenediamine	Sigma, Germany
Tris-base	Sigma Germany

APPENDIX B: EQUIPMENTS

Table B.1: Equipments used in this study

Equipment	Company
Autoclave	ASTEEL SWIFTCLAVE, UK
Balance	Precisa BJ210C
Centrifuge	Beckman Coulter, Allegra X-12, USA Beckman Coulter Allegra X-30R, USA
CO ₂ incubator	Steri Cycle i60, Thermo Fisher Scientific, USA
Deepfreeze	-150°C, Thermo Fisher Scientific, USA -80°C, Binder, USA -20°C, Bosch, Turkey
Electrophoresis Apparatus	Thermo Fisher Scientific, EC1000_90 PowerSupply, USA Thermo Fisher Scientific, MIDICELL PRIMO, USA
Filters	Molgen, Turkey
Flow cytometer	BD Accuri™ Flow Cytometer, USA BD FACSCalibur Flow Cytometer™, USA BD Influx™ Cell Sorter, USA
Gel Documentation	BIO-RAD, USA
Heater/Stirrer	Yellow Line, USA
Ice Machine	Scotsman Inc., USA
Laminar Flow	Thermo Fisher Scientific SDFE2020, USA
Liquid Nitrogen Tank	Taylor-Wharton, 3000RS, USA
Microliter Pipettes	Axygen, USA
Microscope	Zeiss, Primo Vert, Germany

Table B.1: Equipments used in this study (cont.)

Microcentrifuge	Beckman Coulter Microfuge 16, USA GILSON GmCLab Capsulefuge PMC-880,USA Mikro200R, Hetich, Germany
Microwave Oven	Beko, Turkey
pH meter	Hanna HI 2020 Edge (R), USA
Refrigerator	Bosch, Turkey Arçelik, Turkey
Spectrophotometer	Beckman Coulter DU730, USA NanoDrop™ 2000, Thermo Fisher Scientific, USA
Thermal Shaker	Thermal Shake Lite VWR, USA
xCELLigence RTCA	ACEA, USA
Vortex	Clifton™ Cyclone Vortex Mixers, USA
Waterbath	Memmert Water Bath, Germany

APPENDIX C: ADAPTATIONS

- Figure 1.1, 1.3, 1.4, and 1.5 was created using BioRender.com
- Figure 1.2 was adapted from “TCR Downstream Signaling” by BioRender.com (2022) and retrieved from <https://app.biorender.com/biorender-templates>.

APPENDIX D: PLASMID MAPS

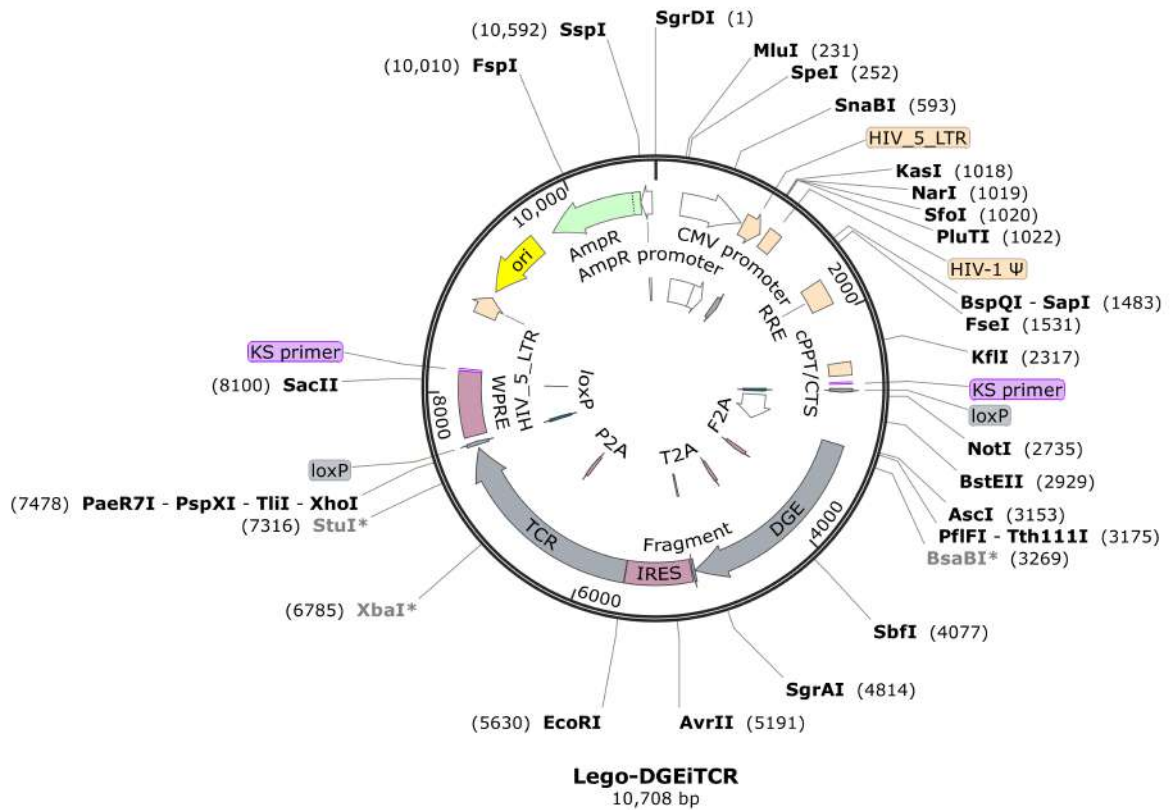


Figure D.1. The plasmid map of Lego-DGEiTCR.

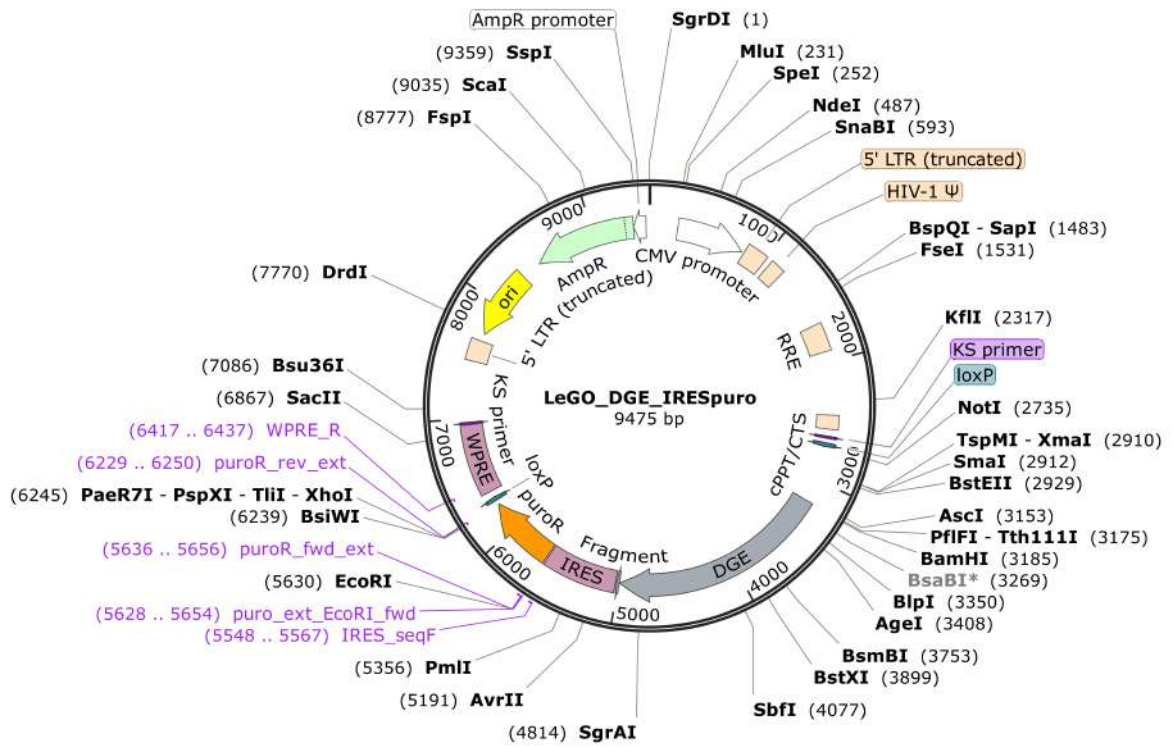


Figure D.2. The plasmid map of LeGO-DGE-IRESpuro.

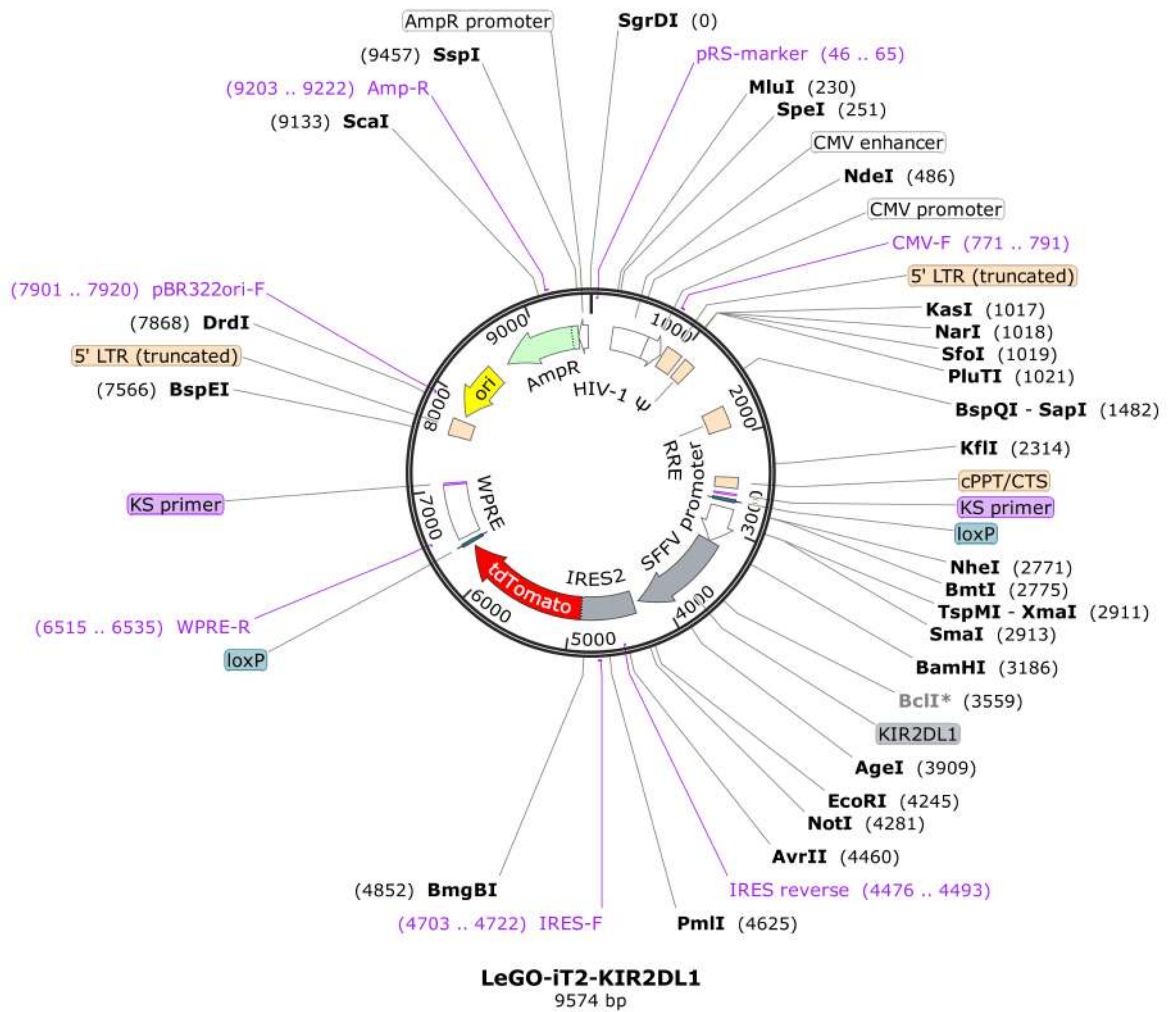


Figure D.3. The plasmid map of LeGO-KIR2DL1-iT2

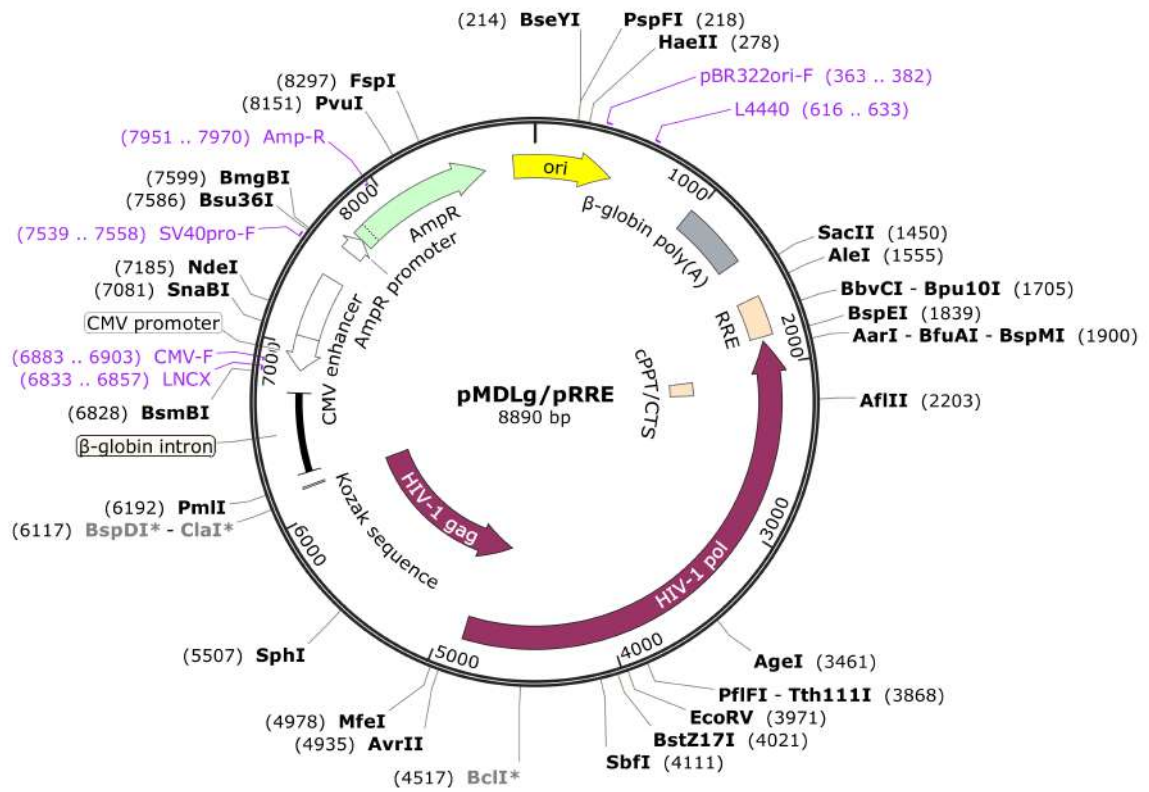


Figure D.4. The plasmid map of pMDLg/gpRRE.

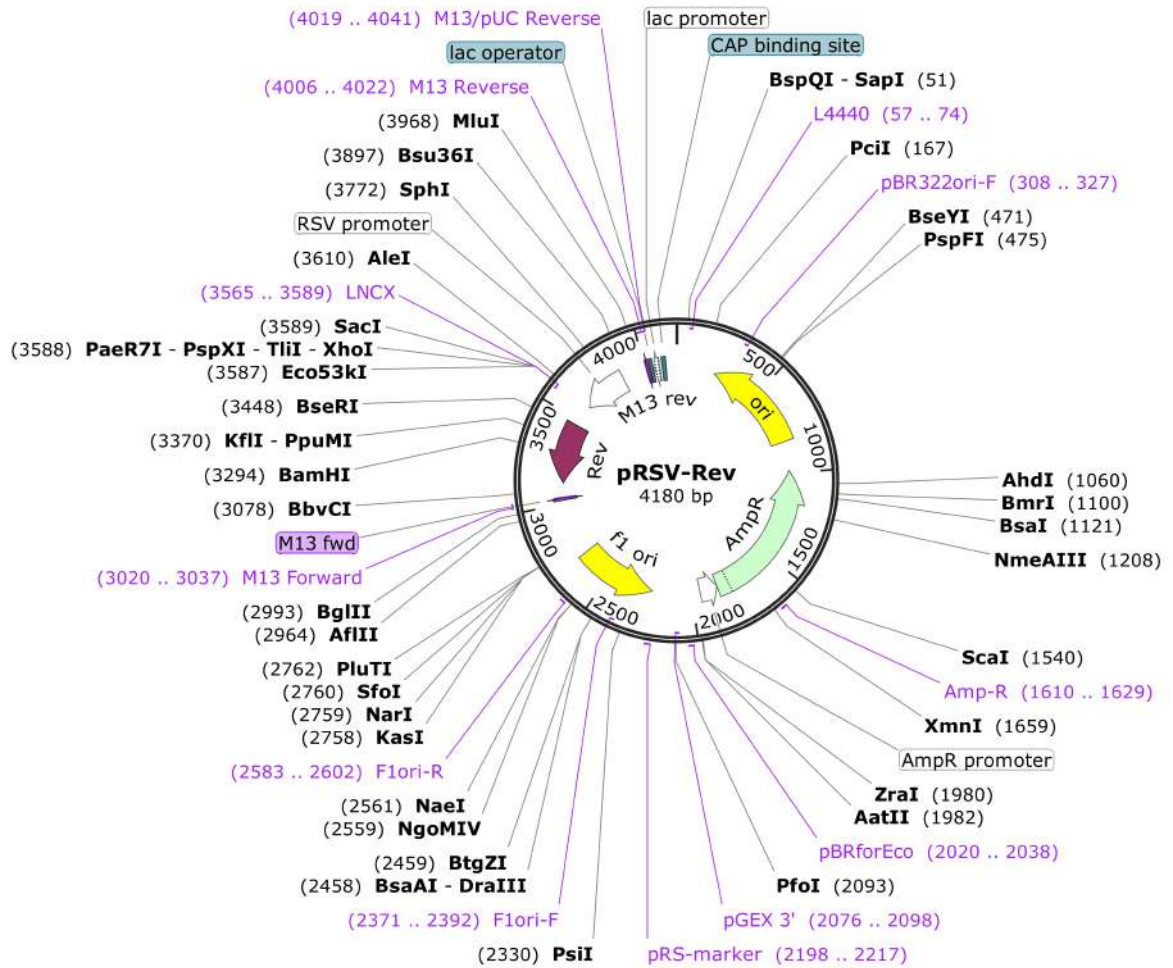


Figure D.5. The plasmid map of pRSV-Rev.

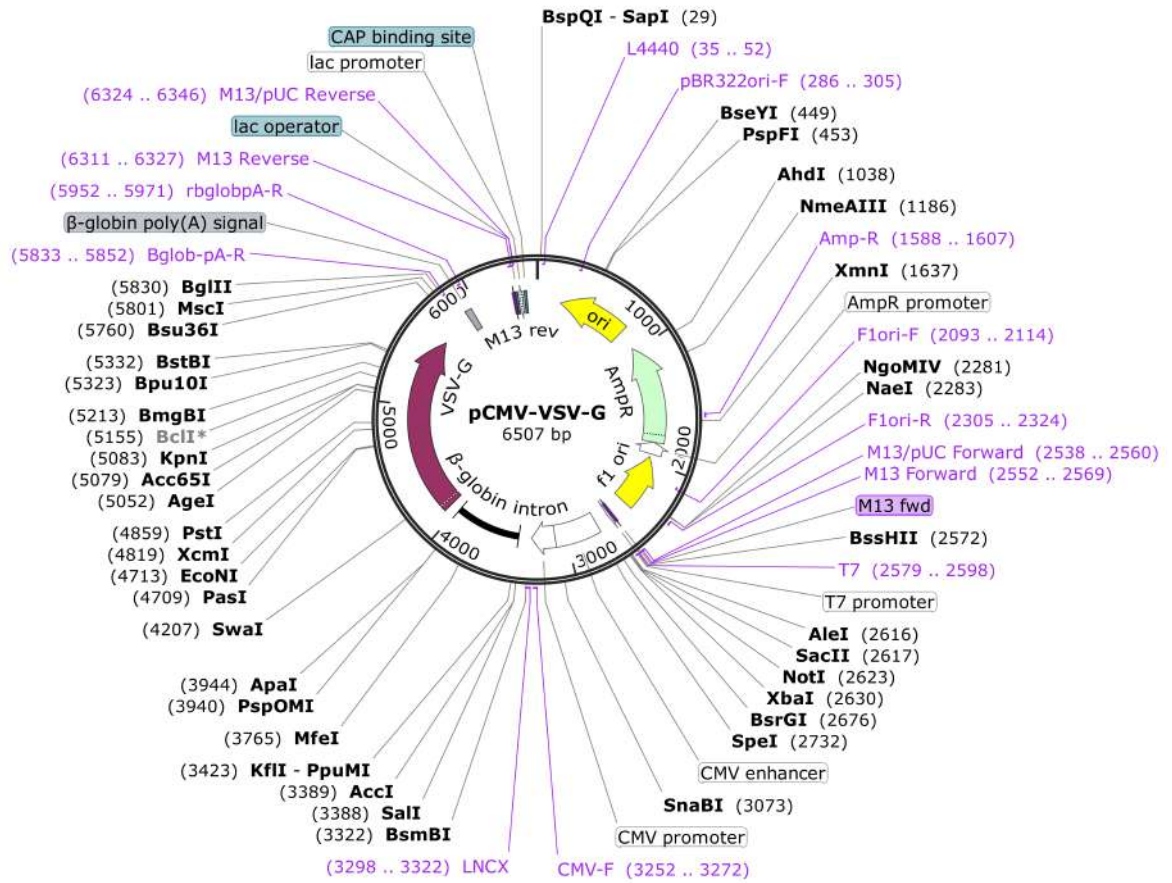


Figure D.6. The plasmid map of pCMV-VSV-G.

APPENDIX E: DNA LADDER

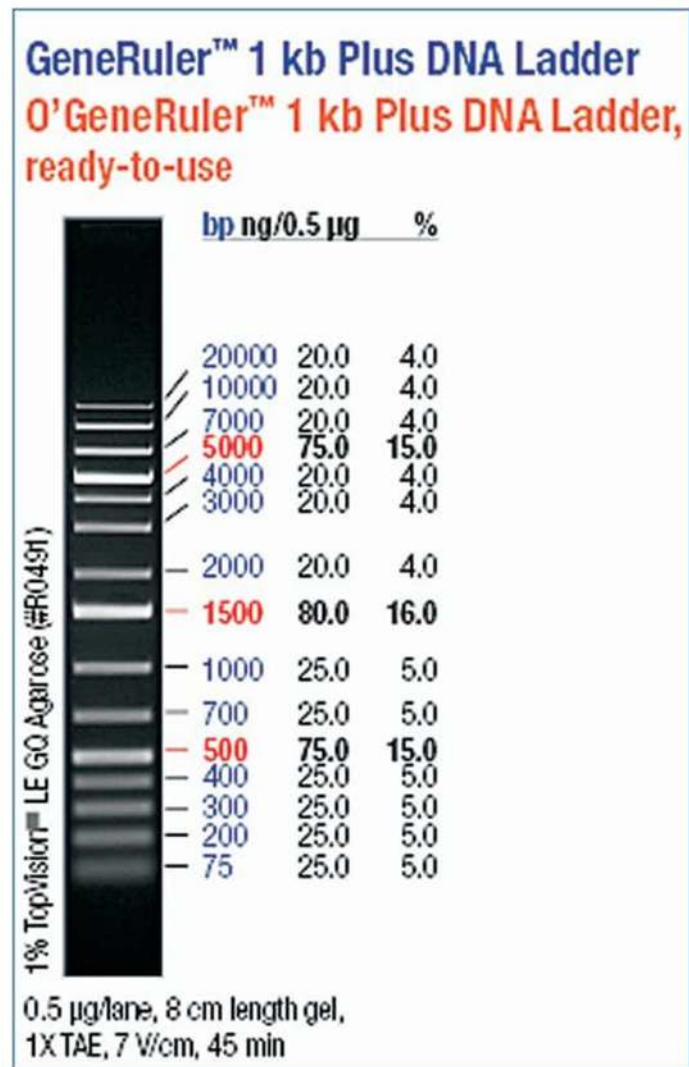


Figure E.1. DNA ladder

APPENDIX F: PROTEIN LADDER

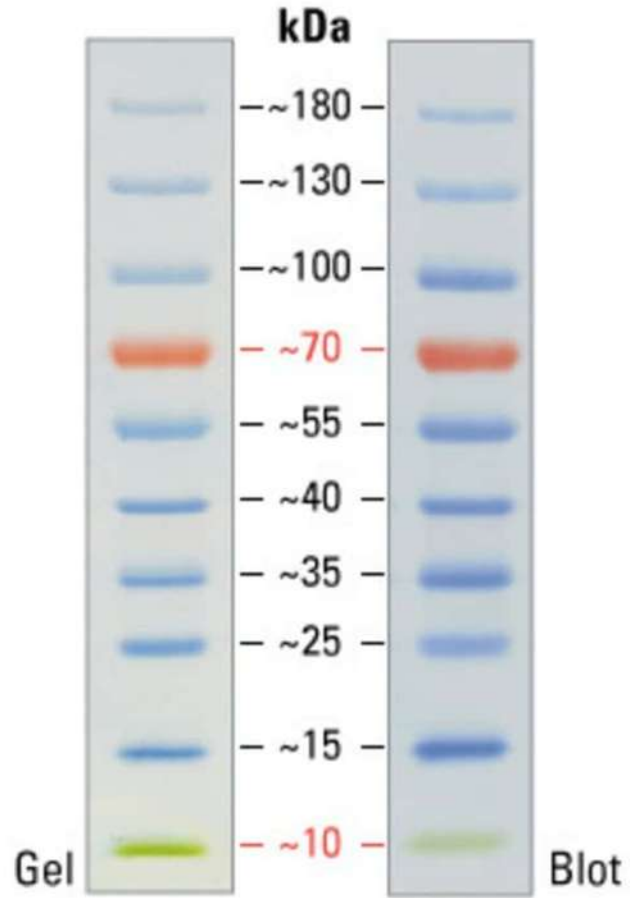


Figure F.1. Protein ladder